

AD A 092143

**LEVEL**

12

DNA 4825F

**FAB CODE COMPUTATIONS OF A 1-KT  
NUCLEAR FREE-AIR BLAST WAVE TO  
LOW SHOCK OVERPRESSURES**

Kaman AviDyne  
83 Second Avenue  
Burlington, Massachusetts 01803

DTIC  
NOV 25 1980  
C

31 January 1979

Final Report for Period 1 August 1978—31 January 1979

CONTRACT No. DNA 001-78-C-0374

APPROVED FOR PUBLIC RELEASE;  
DISTRIBUTION UNLIMITED.

THIS WORK SPONSORED BY THE DEFENSE NUCLEAR AGENCY  
UNDER RDT&E RMSS CODE B342078464 N99QAXAG11108 H2590D.

Prepared for  
Director  
DEFENSE NUCLEAR AGENCY  
Washington, D. C. 20305

DDC FILE COPY

8017 14 037

Destroy this report when it is no longer  
needed. Do not return to sender.

PLEASE NOTIFY THE DEFENSE NUCLEAR AGENCY,  
ATTN: STTI, WASHINGTON, D.C. 20305, IF  
YOUR ADDRESS IS INCORRECT, IF YOU WISH TO  
BE DELETED FROM THE DISTRIBUTION LIST, OR  
IF THE ADDRESSEE IS NO LONGER EMPLOYED BY  
YOUR ORGANIZATION.



UNCLASSIFIED

SECURITY CLASSIFICATION OF THIS PAGE (When Data Entered)

<b>19</b> REPORT DOCUMENTATION PAGE		READ INSTRUCTIONS BEFORE COMPLETING FORM	
<b>18</b> 1. REPORT NUMBER DNA 4825F	2. GOVT ACCESSION NO. AD-A092 143	3. RECIPIENT'S CATALOG NUMBER	
<b>6</b> 4. TITLE (and Subtitle) FAB CODE COMPUTATIONS OF A 1-KT NUCLEAR FREE-AIR BLAST WAVE TO LOW SHOCK OVERPRESSURES		<b>9</b> 5. TYPE OF REPORT & PERIOD COVERED Final Report, <del>for Period</del> 1 August 1978-31 January 1979	
7. AUTHOR Robert F. Smiley J. Ray Ruetenik Michael A. Tomayko		<b>14</b> 6. PERFORMING ORG. REPORT NUMBER KA-TR-158	
9. PERFORMING ORGANIZATION NAME AND ADDRESS Kaman Avidyne 83 Second Avenue Burlington, Massachusetts 01803		<b>15</b> 8. CONTRACT OR GRANT NUMBER(S) DNA 001-78-C-0374	
11. CONTROLLING OFFICE NAME AND ADDRESS Director Defense Nuclear Agency Washington, DC 20305		<b>11</b> 10. PROGRAM ELEMENT, PROJECT, TASK AREA & UNIT NUMBERS Subtask N99QAXAG111-08	
14. MONITORING AGENCY NAME & ADDRESS (if different from Controlling Office) <b>12</b> 58		<b>11</b> 12. REPORT DATE 31 January 1979	
		<b>17</b> 13. NUMBER OF PAGES 58	
		15. SECURITY CLASS. (of this report) UNCLASSIFIED	
		15a. DECLASSIFICATION DOWNGRADING SCHEDULE	
16. DISTRIBUTION STATEMENT (of this Report) Approved for public release; distribution unlimited.			
17. DISTRIBUTION STATEMENT (of the abstract entered in Block 20 if different from Report)			
18. SUPPLEMENTARY NOTES This work sponsored by the Defense Nuclear Agency under RDT&E RMSS Code B342078464 N99QAXAG11108 H2590D.			
19. KEY WORDS (Continue on reverse side if necessary and identify by block number) Nuclear Explosions                      Shock                      Explosions Hydrodynamic Computer Code            Overpressure Blast    Computer Simulation			
20. ABSTRACT (Continue on reverse side if necessary and identify by block number) The FAB hydrodynamic computer code was developed for computing the blast flow characteristics of a nuclear free-air blast wave. The flow field is represented by a multi-cell moving grid with fluid properties calculated by Godunov's method. The shock wave at the blast front is represented by the Hugoniot relation. Real air properties may be represented by either Brode (1965) or Doan-Nickel equations of state. Thermal radiation is taken into account.			

194970

Handwritten signature

UNCLASSIFIED

SECURITY CLASSIFICATION OF THIS PAGE(When Data Entered)

20. ABSTRACT (Continued)

Calculation results are presented and compared with nuclear test data summaries and with other predictions. Predicted FAB shock front overpressures below 10 psi are generally near to or between the extremes of the nuclear test data summaries in DASA 1200 as obtained from ground-based and airborne measurements.

UNCLASSIFIED

SECURITY CLASSIFICATION OF THIS PAGE(When Data Entered)

# PREFACE

This work was performed by the Avidyne Division of the Kaman Sciences Corporation for the Defense Nuclear Agency under Contract DNA 001-78-C-0374. Mr. James F. Moulton, Jr., Chief, Aerospace Systems Division, Shock Physics Director, DNA, served as technical monitor.

Dr. J. Ray Ruetenik of Kaman Avidyne was the project leader under Dr. Norman P. Hobbs, Technical Director of KA.

Appreciation is expressed to Mr. Moulton for his continuing interest and significant support of this program.

<b>Accession For</b>		<input checked="" type="checkbox"/>
NTIS GRA&I		<input type="checkbox"/>
DTIC TAB		<input type="checkbox"/>
Unannounced		
Justification		
By _____		
Distribution/		
Availability Codes		
Dist	Avail and/or	Special
A		

CONVERSION FACTORS FOR U.S. CUSTOMARY  
TO METRIC (SI) UNITS OF MEASUREMENT.

To Convert From	To	Multiply By
angstrom	meters (m)	1.000 000 X E -10
atmosphere (normal)	kilo pascal (kPa)	1.013 25 X E +2
bar	kilo pascal (kPa)	1.000 000 X E +2
barn	meter <sup>2</sup> (m <sup>2</sup> )	1.000 000 X E -28
British thermal unit (thermochemical)	joule (J)	1.054 350 X E +3
calorie (thermochemical)	joule (J)	4.184 000
cal (thermochemical)/cm <sup>2</sup>	mega joule/m <sup>2</sup> (MJ/m <sup>2</sup> )	4.184 000 X E -2
curie	giga becquerel (GBq)**	3.700 000 X E +1
degree (angle)	radian (rad)	1.745 329 X E -2
degree Fahrenheit	degree kelvin (K)	$T_K = (t_F + 459.67)/1.8$
electron volt	joule (J)	1.602 19 X E -19
erg	joule (J)	1.000 000 X E -7
erg/second	watt (W)	1.000 000 X E -7
foot	meter (m)	3.048 000 X E -1
foot-pound-force	joule (J)	1.355 818
gallon (U.S. liquid)	meter <sup>3</sup> (m <sup>3</sup> )	3.785 412 X E -3
inch	meter (m)	2.540 000 X E -2
jerk	joule (J)	1.000 000 X E +9
joule/kilogram (J/kg) (radiation dose absorbed)	Gray (Gy)**	1.000 000
kilotons	terajoules	4.183
kip (1000 lbf)	newton (N)	4.448 222 X E +3
kip/inch <sup>2</sup> (ksi)	kilo pascal (kPa)	6.894 757 X E +3
ktap	newton-second/m <sup>2</sup> (N-s/m <sup>2</sup> )	1.000 000 X E +2
micron	meter (m)	1.000 000 X E -6
mil	meter (m)	2.540 000 X E -5
mile (international)	meter (m)	1.609 344 X E +3
ounce	kilogram (kg)	2.834 952 X E -2
pound-force (lbf avoirdupois)	newton (N)	4.448 222
pound-force inch	newton-meter (N·m)	1.129 848 X E -1
pound-force/inch	newton/meter (N/m)	1.751 268 X E +2
pound-force/foot <sup>2</sup>	kilo pascal (kPa)	4.788 026 X E -2
pound-force/inch <sup>2</sup> (psi)	kilo pascal (kPa)	6.894 757
pound-mass (lbm avoirdupois)	kilogram (kg)	4.535 924 X E -1
pound-mass-foot <sup>2</sup> (moment of inertia)	kilogram-meter <sup>2</sup> (kg·m <sup>2</sup> )	4.214 011 X E -2
pound-mass/foot <sup>3</sup>	kilogram/meter <sup>3</sup> (kg/m <sup>3</sup> )	1.601 846 X E +1
rad (radiation dose absorbed)	Gray (Gy)**	1.000 000 X E -2
roentgen	coulomb/kilogram (C/kg)	2.579 760 X E -4
shake	second (s)	1.000 000 X E -8
slug	kilogram (kg)	1.459 390 X E +1
torr (mm Hg, 0° C)	kilo pascal (kPa)	1.333 22 X E -1

\*The becquerel (Bq) is the SI unit of radioactivity; 1 Bq = 1 event/s.  
\*\*The Gray (Gy) is the SI unit of absorbed radiation.

A more complete listing of conversions may be found in "Metric Practice Guide E 380-74," American Society for Testing and Materials.

# TABLE OF CONTENTS

<u>Section</u>	<u>Page</u>
LIST OF ILLUSTRATIONS- - - - -	4
LIST OF TABLES - - - - -	5
1 INTRODUCTION - - - - -	7
2 BACKGROUND - - - - -	8
3 THE FAB CODE - - - - -	10
4 FAB CODE RUNS - - - - -	13
4-1 Cell Configurations - - - - -	13
4-2 Code Results for 273 Cell Configurations- - - - -	13
4-3 Comparison of 134 and 273 Cell Results- - - - -	24
5 COMPARISONS WITH OTHER PREDICTIONS AND TEST DATA - -	37
5-1 Shock Front Pressures - - - - -	37
5-1.1 Equation-of-state - - - - -	37
5-1.2 Initial Conditions - - - - -	37
5-1.3 Comparisons with Nuclear Test Data Summaries - - - - -	48
5-1.4 Thermal Radiation - - - - -	49
5-1.5 Shock Arrival Time - - - - -	49
5-2 Pressure, Density and Velocity Distributions -	50
6 CONCLUSIONS- - - - -	51
7 REFERENCES - - - - -	53

## LIST OF ILLUSTRATIONS

<u>Figure</u>		<u>Page</u>
1	Sketch illustrating the FAB model - - - - -	11
2	Comparison of shock front pressures - - - - -	22
3	Comparisons of pressure, density and velocity distributions at 0.010 seconds after detonation - - -	25
4	Comparisons of pressure, density and velocity distributions at 0.102 seconds after detonation - - -	28
5	Comparisons of pressure, density and velocity distributions at 1.020 seconds after detonation - - -	31
6	Comparisons of pressure, density and velocity distributions at 10.32 seconds after detonation - - -	34

# LIST OF TABLES

<u>Table</u>		<u>Page</u>
1	Principal FAB code runs - - - - -	14
2	Cell configurations for FAB code runs - - - - -	15
3	Code results for Run FAB-273-5 - - - - -	16
4	Code results for Run FAB-273-7 - - - - -	19
5	Comparison of shock front pressures - - - - -	38
6	Effect of initial conditions on shock front pressures	40
7	Effect of initial conditions on scaled shock front pressures - - - - -	42
8	Effect of thermal radiation on shock front pressures	44
9	Comparison of shock arrival times - - - - -	46

# SECTION 1

## INTRODUCTION

The various existing predictions of free-air nuclear blast wave properties for low overpressures (e.g., Refs. 1 to 7) have had unresolved differences that have been of concern to the technical community for a number of years. When these differing predictions are employed as inputs to techniques used for the formulation of height-of-burst charts at low shock overpressures, the differences become magnified. That is, the resulting height-of-burst curves differ to even a markedly greater degree.

A principal question concerning these prediction methods is the deterioration of the predicted properties near the shock front at low shock overpressures. Most distributions of predicted overpressure, for example, exhibit a pressure rise at the blast front that is smeared over a considerable distance, differing significantly from the characteristic sharp rise and smooth decay of measured blast waves.

In order to provide a blast prediction method of improved accuracy for the low overpressure range which does not smear the blast front, Kaman Avidyne developed for the Defense Nuclear Agency the FAB (free-air-burst) hydrocode, described herein, which represents the blast front as a Hugoniot shock wave. This code was developed in a manner similar to that for the REFLECT code developed by KA for DNA for computer computation of the ground reflection of a free-air nuclear blast wave (Ref. 8).

Section 2 of this report briefly discusses some background information on the free-air-blast problem, with respect to existing code predictions and experimental data. Section 3 describes the major features of the FAB code and Section 4 presents results from the principal code runs made. Section 5 presents a discussion of the FAB code results with respect to other predictions and test data. Conclusions are presented in Section 6.

## SECTION 2

### BACKGROUND

This section briefly reviews some features and limitations of the existing test data and methods of predicting free-air-blast conditions, with particular attention to the low overpressure range from about 7 to 0.3 psi.

First, considering the nuclear test data for the variation of shock front overpressure with range, there are several useful data summaries (Ref. 2). Ground based nuclear test measurements from tower gages and event photography are represented by the U.S.-'59 empirical curve (Ref. 2), which is used as one basis for comparisons in this report. Airborne measurements from gages mounted on aircraft and in canisters have been represented by various polynomials (Ref. 2). A convenient summary table of these airborne measurements which is used as a basis for comparisons in this report is given in Table 3.2-6 of Reference 2. Generally in the low pressure range below 5 psi the airborne data indicate higher overpressures than the ground based data, with differences of about 15 percent at the 2 psi level. No satisfactory explanation for these differences has yet been established.

With regard to theoretical predictions, there are available a number of useful codes and numerical results, such as the M-problem (Ref. 2), Brode's point source solution (Ref. 1), the Hull code (Ref. 3), the AFWL Revised Nuclear Blast Standard code (Ref. 7) and the NOL code (Refs. 4 and 5). These various codes have all produced useful results, roughly in agreement with the test data. However, for high accuracy at low overpressures these code results are generally somewhat suspect because of their inability to achieve accurate resolution of blast wave properties at the blast front. Because of inherent instability of these numerical methods, either artificial viscosity or equivalent numerical differencing methods have been employed. Artificial viscosity results in the smearing of shock waves into a compression wave instead of a

2

shock wave. To steepen compression waves, methods using artificial viscosity have resorted to fine mesh spacing. This has improved the pressure distributions insofar as the extent of the compression wave has been reduced and the peak pressure has increased. Unfortunately to reduce the cell size to anything approaching the thickness of a shock wave would result in prohibitive computer times. Extrapolation schemes have been employed for extrapolation of the computed profiles to a point within the compression wave for assigning shock properties. But the extrapolations become particularly large at low shock overpressures.

In view of these problems, there does not appear to exist in the literature an analytical procedure for calculating free-air-burst shock front characteristics in the low pressure range with a high enough accuracy to resolve the existing questions of significant differences between ground based and airborne nuclear test measurements.

## SECTION 3

### THE FAB CODE

The FAB computer code was developed to solve the spherically symmetrical one-dimensional transient fluid-flow problem of the expansion of an initially prescribed flow into an initially undisturbed uniform atmosphere. In the present application this code deals specifically with the problem of modeling the fluid flow produced by the detonation of a 1KT nuclear explosion in a uniform sea-level atmosphere.

The code computes the flow in a moving cell coordinate system similar to the one shown in Figure 1. The cells are symmetrical with respect to the origin of coordinates, so that each cell represents a spherical shell region, initially prescribed by any arbitrary inner and outer radii. The outer boundary of the cell system represents the outer limit of the disturbed flow region, which is initially specified and grows radially thereafter at the speed of the shock wave created between the outermost cell of the disturbed region and the outer undisturbed atmosphere.

All inner cell radial boundaries are taken to increase similarly, at speeds proportional to the ratio of their initial radial distances from the origin of coordinates to the initial shock front radius.

The flow between adjacent cells in the moving coordinate system is computed using the Godunov technique (e.g., see Ref. 9 or 10) in the manner previously used in nuclear blast-field calculations by Thompson and Ruetenik (Ref. 8). More specifically, in the interior of the disturbed region, the flux conditions at cell boundaries are computed as locally isentropic shock-expansion phenomena for large pressure and velocity differences between cells, using an isentropic exponent ( $\gamma_e = (d \ln(p) / d \ln(\rho))_s$ ) which is the average of the values for the two adjacent cells; for small pressure and velocity differences between adjacent cells a linearized approximation is used. For the outermost

UNDISTURBED ATMOSPHERIC CONDITIONS

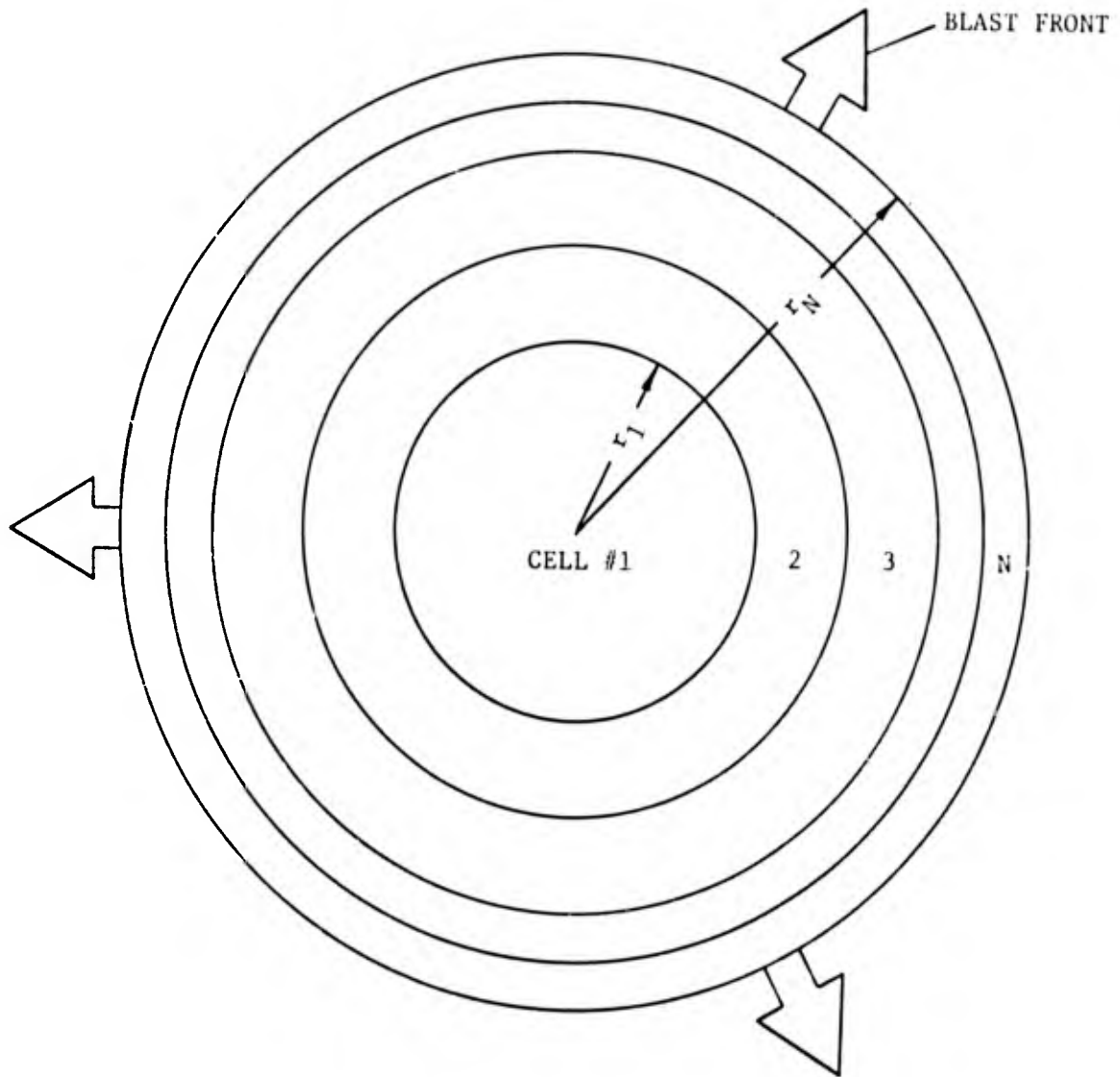


Figure 1. Sketch illustrating the FAB model.

cell boundary of the disturbed region, the shock front velocity and associated fluxes are calculated on the basis of the exact Hugoniot relationships for a real gas.

The code assumes a real air medium with thermodynamic equation-of-state properties given by a choice of two analytical representations, designated as Brode 1965 (Ref. 11) and Doan-Nickel (Ref. 7, see AIR subroutine).

In addition to hydrodynamic phenomena, the code takes into account the thermal radiation of a nuclear (1KT) blast, with the total radiation flux computed as a function of time according to Reference 12 and the spatial distribution of radiated energy being calculated according to the model used in Reference 6.

Input to the code consists of the specification of the initial pressure, density and velocity in the entire disturbed fluid field or, alternatively, the specification of density, internal energy and velocity. In the former case, initial conditions are generated from early-time predictions of the AFWL Nuclear Blast Standard (1KT) code (Ref. 7); in the second case inputs may be prepared from Sputter code results (e.g., Ref. 13).

Program output consists of tables of pressure, density and velocity printouts for selected times.

The FAB code has been run primarily on a CDC CYBER 176 computer. The code has a core requirement of 117K octal for a 1000 cell configuration. Approximately 10 CP minutes are required for a complete run with 273 cells.

## SECTION 4

### FAB CODE RUNS

This section describes and lists the principal FAB code runs made, presents the numerical results obtained for two runs with 273 cell configurations and discusses some factors related to code accuracy.

#### 4-1 CELL CONFIGURATIONS.

Runs were made with the FAB code for a variety of conditions with either a 134 or 273 cell configuration. The runs of principal interest are listed in Table 1. The cell sizes used in these runs are listed in Table 2, where cell radial widths are listed in order of increasing distance from the origin of coordinates. These cell sizes were selected so that absolute pressure changes between adjacent cells were generally less than 2 percent for the 134 cell case and less than 1 percent for the 273 cell case.

Near the shock front absolute pressure changes between adjacent cells were generally less than the above values. In terms of percent of shock front overpressure, the pressure changes between adjacent cells in this region were generally less than 1.2 percent for the 134 cell configuration and less than 0.6 percent for the 273 cell configuration. For shock front overpressures below 1 psi the percentage changes were greater but the pressure differences between adjacent cells here were generally below 0.01 psi.

#### 4-2 CODE RESULTS FOR 273 CELL CONFIGURATION.

Results of the principal FAB code runs for the 273 cell configuration are presented in Tables 3 and 4, for Runs 273-5 and 273-7, corresponding to Brode and Doan-Nickel equations-of-state, respectively. The tables present values of shock front radius, shock front overpressure (FAB) and shock arrival time for radii from about 150 to 23,000 feet and for overpressures from 543 to 0.1 psi. These same shock front overpressure data are also shown in Figure 2. In addition to the FAB code results, Tables 3 and 4 also present calculated overpressures for the same radii according to the AFWL Revised 1-KT-Standard (Ref. 7).

Table 1

PRINCIPAL FAB CODE RUNS<sup>a</sup>

RUN NO.	NO. CELLS	INPUT <sup>b</sup>	YIELD (KT) <sup>d</sup>	EQ. OF STATE
134-18	134	AFWL-1KT-STD-REV	1.028	Brode
134-19	134	SPUTTER FB21	0.994	Brode
134-20	134	AFWL-1KT-STD-REV	1.011	Doan-Nickel
134-21	134	AFWL-1KT-STD-REV	1.025	Brode <sup>c</sup>
273-5	273	AFWL-1KT-STD-REV	1.028	Brode
273-7	273	AFWL-1KT-STD-REV	1.010	Doan-Nickel

<sup>a</sup>All code runs made for ambient atmosphere conditions of 2117 psfa and 0.002378 slug/ft<sup>3</sup>.

<sup>b</sup>All inputs for a nominal 1 KT detonation; initial conditions specified at 0.01 second after detonation.

<sup>c</sup>Thermal radiation neglected in Run 134-21 only.

<sup>d</sup>Yields computed on the basis of 1KT = 4.189 x 10<sup>19</sup> erg. Yields are the sum of gas internal energy and kinetic energy at 0.01 seconds and thermal energy radiated to this time. Yields given are dependent upon the particular equation of state used and accuracy of the input.

Table 2  
CELL CONFIGURATIONS FOR FAB CODE RUNS

CELL RADIAL WIDTH (PERCENT OUTER RADIUS)	NO. CELLS THIS WIDTH
134 cell case	
10 <sup>a</sup>	2
5	4
2.5	8
1.25	8
.833	12
.40	25
.20	25
.10 <sup>b</sup>	50
273 cell case	
2.5 <sup>a</sup>	16
1.25	16
.625	16
.40	25
.20	50
.10	50
.05 <sup>b</sup>	100

<sup>a</sup>Innermost cells

<sup>b</sup>Outermost cells

Table 3.

CODE RESULTS FOR RUN FAB-273-5

(Brode Equation of State)

RADIUS (FT)	SHOCK FRONT OVERPRESSURE (PSI)		FAB BLAST ARRIVAL TIME (SEC)
	FAB	1KT-STD	
153.6	541.637	543.315	.0100
168.4	414.412	421.363	.0125
184.0	323.472	330.779	.0155
200.5	255.442	262.103	.0190
218.3	202.619	208.759	.0233
237.1	162.425	167.739	.0283
257.0	131.659	136.074	.0341
277.7	107.861	111.506	.0407
299.3	89.290	92.351	.0482
321.4	74.601	77.310	.0565
344.3	62.758	65.380	.0657
367.7	53.416	55.791	.0757
391.7	45.516	48.077	.0866
416.2	39.182	41.747	.0985
441.4	34.076	36.510	.1112
467.2	29.943	32.148	.1249
493.6	26.564	28.489	.1394
520.6	23.754	25.393	.1548
548.2	21.362	22.753	.1711
576.5	19.291	20.486	.1882
605.5	17.479	18.525	.2063
635.2	15.885	16.821	.2252
665.7	14.479	15.331	.2451
696.9	13.236	14.021	.2659
729.0	12.135	12.863	.2877
762.0	11.156	11.836	.3105
795.8	10.284	10.921	.3343
830.6	9.503	10.101	.3591
866.4	8.802	9.365	.3850
903.2	8.171	8.701	.4119
941.0	7.599	8.100	.4400
980.0	7.081	7.555	.4692
1020.2	6.610	7.058	.4997
1061.5	6.176	6.605	.5313
1104.2	5.779	6.190	.5641
1148.1	5.418	5.810	.5983
1193.4	5.085	5.460	.6338
1240.1	4.779	5.137	.6706
1288.2	4.496	4.839	.7089
1337.9	4.234	4.563	.7486
1389.1	3.991	4.308	.7898
1442.0	3.765	4.070	.8326

Table 3. Continued.

CODE RESULTS FOR RUN FAB-273-5

(Brode Equation of State)

RADIUS (FT)	SHOCK FRONT OVERPRESSURE (PSI)		FAB BLAST ARRIVAL TIME (SEC)
	FAB	1KT-STD	
1496.5	3.555	3.849	.8769
1552.8	3.360	3.643	.9229
1610.9	3.177	3.451	.9706
1670.9	3.007	3.271	1.0201
1732.9	2.848	3.103	1.0714
1796.8	2.698	2.945	1.1245
1862.8	2.559	2.797	1.1796
1931.0	2.427	2.658	1.2366
2001.4	2.304	2.527	1.2957
2074.2	2.188	2.404	1.3570
2149.3	2.079	2.288	1.4204
2226.9	1.977	2.178	1.4861
2307.0	1.880	2.075	1.5542
2389.8	1.789	1.977	1.6247
2475.3	1.703	1.885	1.6976
2563.7	1.622	1.797	1.7732
2655.0	1.545	1.714	1.8514
2749.3	1.472	1.636	1.9324
2846.7	1.403	1.561	2.0163
2947.4	1.338	1.490	2.1030
3051.5	1.277	1.423	2.1929
3159.0	1.218	1.360	2.2858
3270.1	1.163	1.299	2.3821
3384.9	1.110	1.241	2.4816
3503.6	1.060	1.186	2.5847
3626.2	1.013	1.134	2.6913
3752.9	.967	1.085	2.8017
3883.9	.925	1.037	2.9159
4019.2	.884	.992	3.0340
4159.1	.845	.949	3.1562
4303.7	.808	.908	3.2827
4453.1	.773	.869	3.4136
4607.5	.740	.832	3.5489
4767.1	.708	.796	3.6889
4932.1	.677	.762	3.8338
5102.6	.648	.730	3.9837
5278.9	.621	.699	4.1387
5461.1	.594	.669	4.2990
5649.4	.569	.641	4.4649
5844.0	.545	.614	4.6364
6045.2	.522	.588	4.8139
6253.1	.500	.564	4.9974

Table 3. Concluded.  
 CODE RESULTS FOR RUN FAB-273-5  
 (Brode Equation of State)

RADIUS (FT)	SHOCK FRONT OVERPRESSURE (PSI)		FAB BLAST ARRIVAL TIME (SEC)
	FAB	1KT-STD	
6468.1	.479	.540	5.1872
6690.3	.459	.517	5.3835
6919.9	.440	.496	5.5866
7157.4	.422	.475	5.7966
7402.8	.405	.456	6.0138
7656.4	.388	.437	6.2384
7918.7	.372	.419	6.4707
8189.7	.357	.402	6.7109
8469.9	.342	.385	6.9593
8759.6	.328	.369	7.2162
9059.0	.315	.354	7.4819
9368.5	.302	.340	7.7567
9688.4	.291	.326	8.0408
10019.2	.280	.313	8.3346
10361.1	.269	.300	8.6384
10714.5	.259	.288	8.9526
11079.9	.249	.276	9.2775
11457.6	.239	.265	9.6134
11848.1	.230	.254	9.9608
12251.7	.221	.244	10.3200
12668.9	.212	.234	10.6914
13100.3	.204	.225	11.0754
13546.2	.196	.216	11.4725
14007.2	.188	.207	11.8831
14483.7	.181	.199	12.3077
14976.3	.174	.191	12.7467
15485.6	.167	.184	13.2006
16012.0	.161	.176	13.6699
16556.2	.154	.169	14.1552
17118.8	.148	.163	14.6569
17700.4	.143	.156	15.1757
18301.7	.137	.150	15.7120
18923.3	.132	.144	16.2666
19565.8	.127	.139	16.8400
20230.1	.122	.133	17.4329
20916.8	.117	.128	18.0458
21626.7	.113	.123	18.6796
22360.5	.108	.118	19.3348
23119.2	.104	.114	20.0123

Table 4.

CODE RESULTS FOR RUN FAB-273-7

(Doan-Nickel Thermodynamics)

RADIUS (FT)	SHOCK FRONT OVERPRESSURE (PSI)		FAB BLAST ARRIVAL TIME (SEC)
	FAB	IKT-STD	
153.6	541.964	543.315	.0100
168.3	414.215	421.742	.0125
183.9	322.958	331.096	.0155
200.4	255.010	262.252	.0190
218.3	202.450	208.791	.0233
237.1	162.413	167.730	.0283
257.0	131.689	136.094	.0341
277.7	107.798	111.586	.0407
299.1	88.994	92.477	.0482
321.2	74.054	77.459	.0565
343.9	62.082	65.537	.0657
367.3	52.434	55.970	.0757
391.2	44.677	48.211	.0867
415.8	38.446	41.852	.0987
441.0	33.428	36.593	.1116
466.8	29.379	32.216	.1254
493.1	26.090	28.545	.1400
520.1	23.369	25.440	.1555
547.7	21.059	22.793	.1719
576.0	19.054	20.518	.1892
605.0	17.293	18.553	.2073
634.8	15.739	16.843	.2264
665.3	14.363	15.349	.2464
696.5	13.141	14.035	.2673
728.7	12.052	12.875	.2892
761.6	11.085	11.846	.3121
795.5	10.220	10.928	.3360
830.3	9.445	10.107	.3609
866.1	8.748	9.370	.3869
902.9	8.119	8.705	.4140
940.8	7.551	8.103	.4422
979.8	7.036	7.557	.4715
1020.0	6.567	7.060	.5020
1061.4	6.138	6.607	.5338
1104.0	5.747	6.192	.5668
1147.9	5.388	5.811	.6011
1193.2	5.058	5.461	.6367
1239.9	4.749	5.138	.6736
1288.1	4.465	4.840	.7120
1337.8	4.205	4.564	.7519
1389.0	3.964	4.308	.7932
1441.9	3.745	4.070	.8361

Table 4. Continued.

CODE RESULTS FOR RUN FAB-273-7  
(Doan-Nickel Thermodynamics)

RADIUS (FT)	SHOCK FRONT OVERPRESSURE (PSI)		FAB BLAST ARRIVAL TIME (SEC)
	FAB	1KT-STD	
1496.5	3.532	3.849	.8806
1552.8	3.338	3.643	.9268
1610.9	3.157	3.451	.9746
1670.9	2.989	3.271	1.0242
1732.8	2.831	3.103	1.0756
1796.8	2.683	2.945	1.1289
1862.8	2.544	2.797	1.1841
1931.0	2.414	2.658	1.2414
2001.5	2.292	2.527	1.3007
2074.2	2.178	2.404	1.3621
2149.3	2.070	2.288	1.4257
2226.9	1.968	2.178	1.4916
2307.1	1.872	2.075	1.5598
2389.9	1.782	1.977	1.6305
2475.5	1.697	1.884	1.7037
2563.8	1.616	1.797	1.7795
2655.2	1.540	1.714	1.8579
2749.5	1.468	1.636	1.9391
2847.0	1.400	1.561	2.0232
2947.7	1.354	1.490	2.1102
3051.9	1.297	1.423	2.2003
3159.5	1.221	1.359	2.2936
3270.6	1.162	1.299	2.3901
3385.5	1.110	1.241	2.4899
3504.2	1.060	1.186	2.5933
3626.9	1.013	1.134	2.7002
3753.7	.969	1.084	2.8108
3884.7	.926	1.037	2.9253
4020.1	.886	.992	3.0438
4160.1	.847	.949	3.1664
4304.7	.811	.908	3.2932
4454.2	.776	.869	3.4244
4608.8	.743	.831	3.5601
4768.5	.711	.796	3.7005
4933.6	.681	.762	3.8458
5104.2	.653	.729	3.9961
5280.6	.625	.698	4.1515
5462.9	.599	.669	4.3123
5651.3	.574	.641	4.4786
5846.1	.550	.614	4.6506
6047.4	.528	.588	4.8285
6255.6	.506	.563	5.0126

Table 4. Concluded.

CODE RESULTS FOR RUN FAB-273-7

(Doan-Nickel Thermodynamics)

RADIUS (FT)	SHOCK FRONT OVERPRESSURE (PSI)		FAB BLAST ARRIVAL TIME (SEC)
	FAB	1KT-STD	
6470.7	.485	.540	5.2029
6693.1	.466	.517	5.3998
6923.0	.447	.496	5.6034
7160.6	.429	.475	5.8140
7406.2	.411	.455	6.0318
7660.1	.395	.437	6.2570
7922.6	.379	.419	6.4900
8193.9	.364	.401	6.7309
8474.4	.349	.385	6.9800
8764.4	.335	.369	7.2377
9064.1	.322	.354	7.5041
9373.9	.310	.339	7.7796
9694.2	.297	.326	8.0645
10025.3	.293	.312	8.3592
10367.6	.286	.300	8.6640

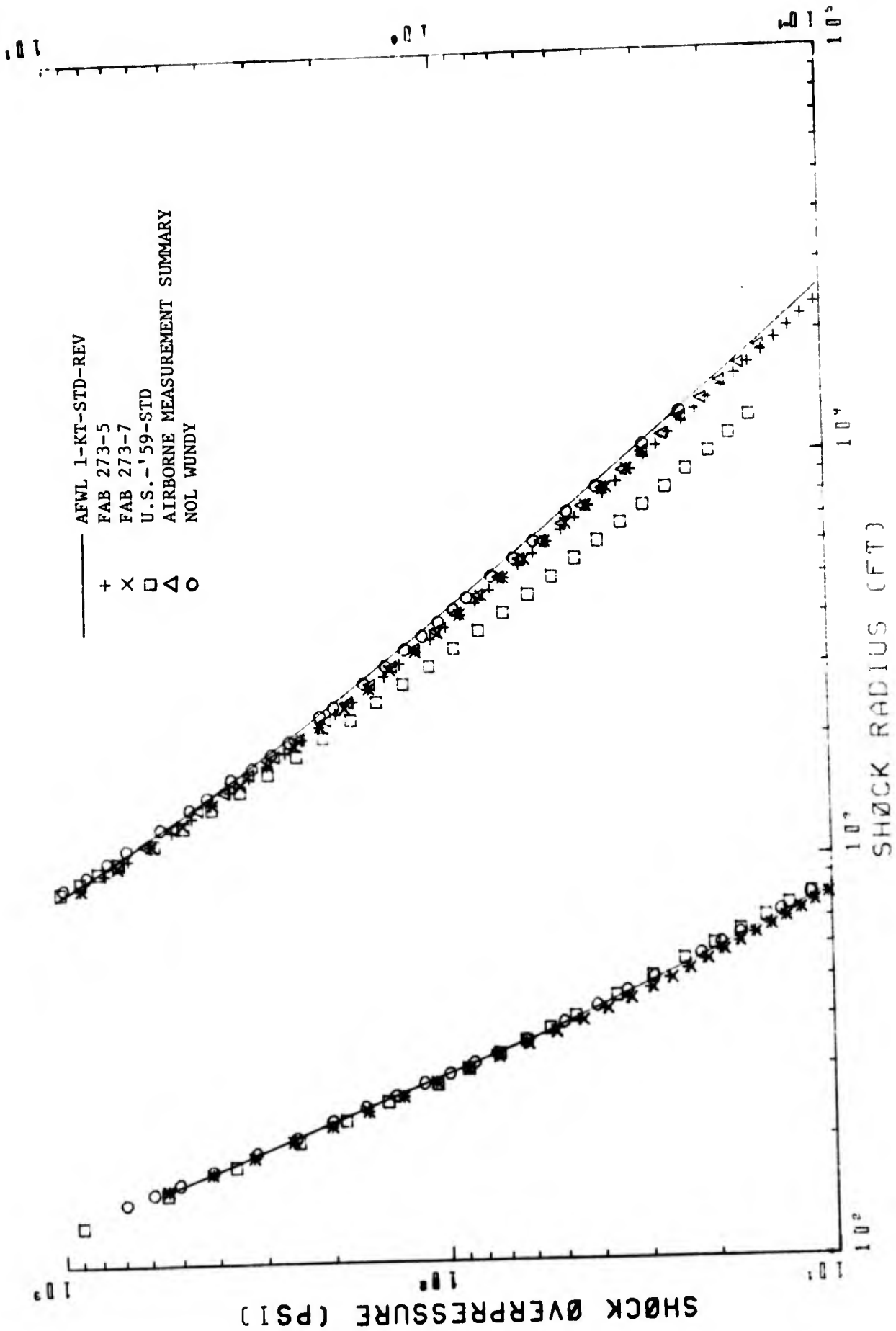


Figure 2. Comparison of Shock Front Pressures.

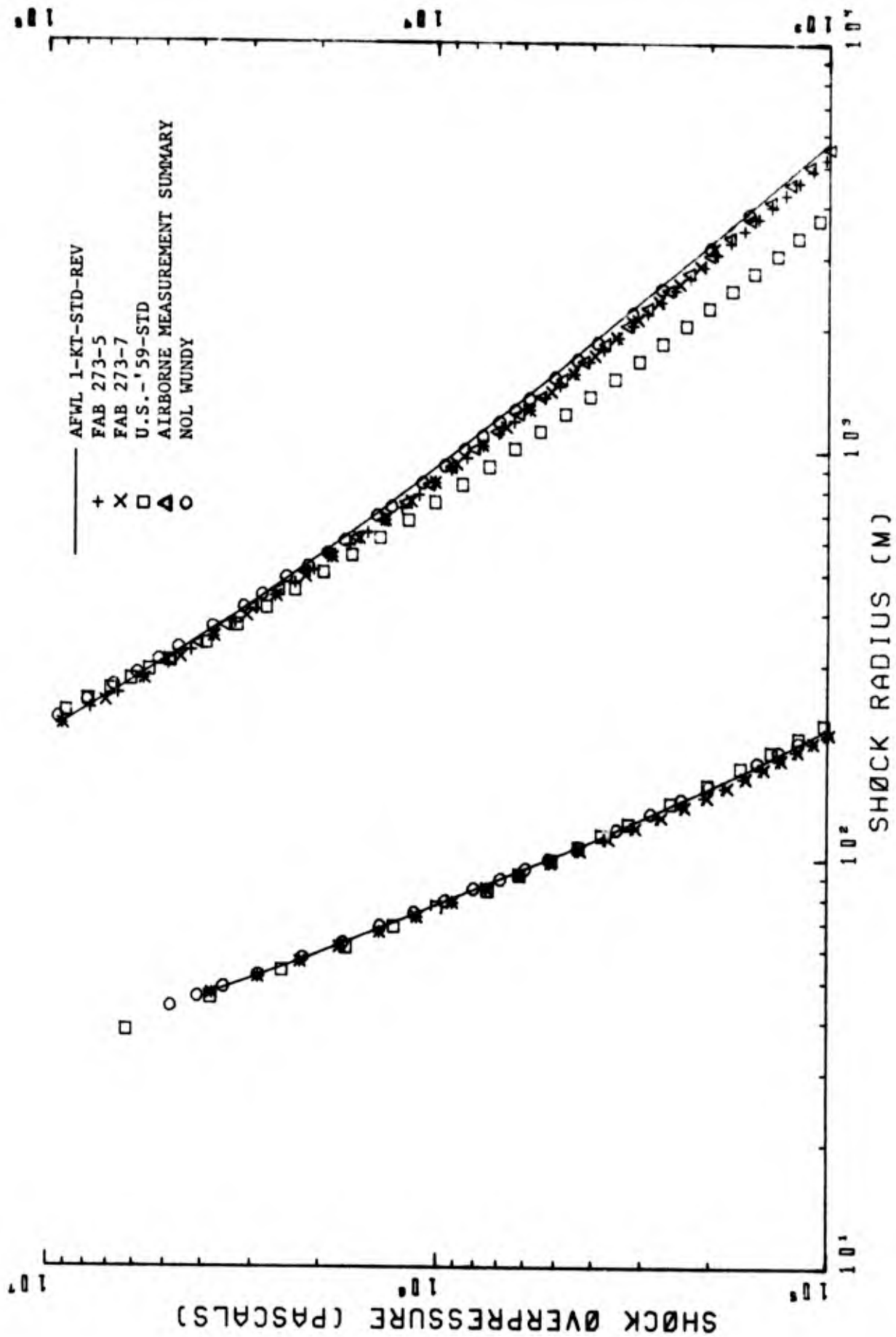


Figure 2. Concluded.

Typical overpressure, overdensity and material velocity distributions in the blast field are presented in Figures 3 to 6 for Run 273-5 for times after detonation of 0.010, 0.102, 1.020 and 10.32 seconds. Also shown in these figures are the corresponding distributions calculated from the AFWL Revised 1-KT Standard (Ref. 7) for the same blast front radius. (Metric units are used in Figures 3 to 6 to permit convenient reference to similar curves in Ref. 7.) The distributions shown in Figure 3 for 0.010 second represent the initial conditions for the FAB computations, which for this run were taken equal to the shown AFWL 1-KT-STD-REV distributions.

The distributions shown in Figures 3 to 6 were computed with use of the Brode (1965) equation-of-state. Essentially the same distributions were obtained from a similar run made with the Doan-Nickel equation-of-state (Run 273-7).

#### 4-3 COMPARISON OF 134 AND 273 CELL RESULTS.

Results from the 134 cells and 273 cell code runs were generally in good agreement with each other. For overpressures above 1 psi, shock front overpressures for the two cases generally agreed within 1 percent and for lower pressures within 0.01 psi. In the lower overpressure range below 1 psi, the 134 cell configuration gave slightly lower shock overpressures, generally in agreement with what would be expected for the larger cell sizes used. In view of these considerations, it appears that the 273 cell results presented in Tables 3 and 4 represent a fine enough cell division such that no significant changes in shock front overpressure would be expected to be obtained by increasing the number of cells further.

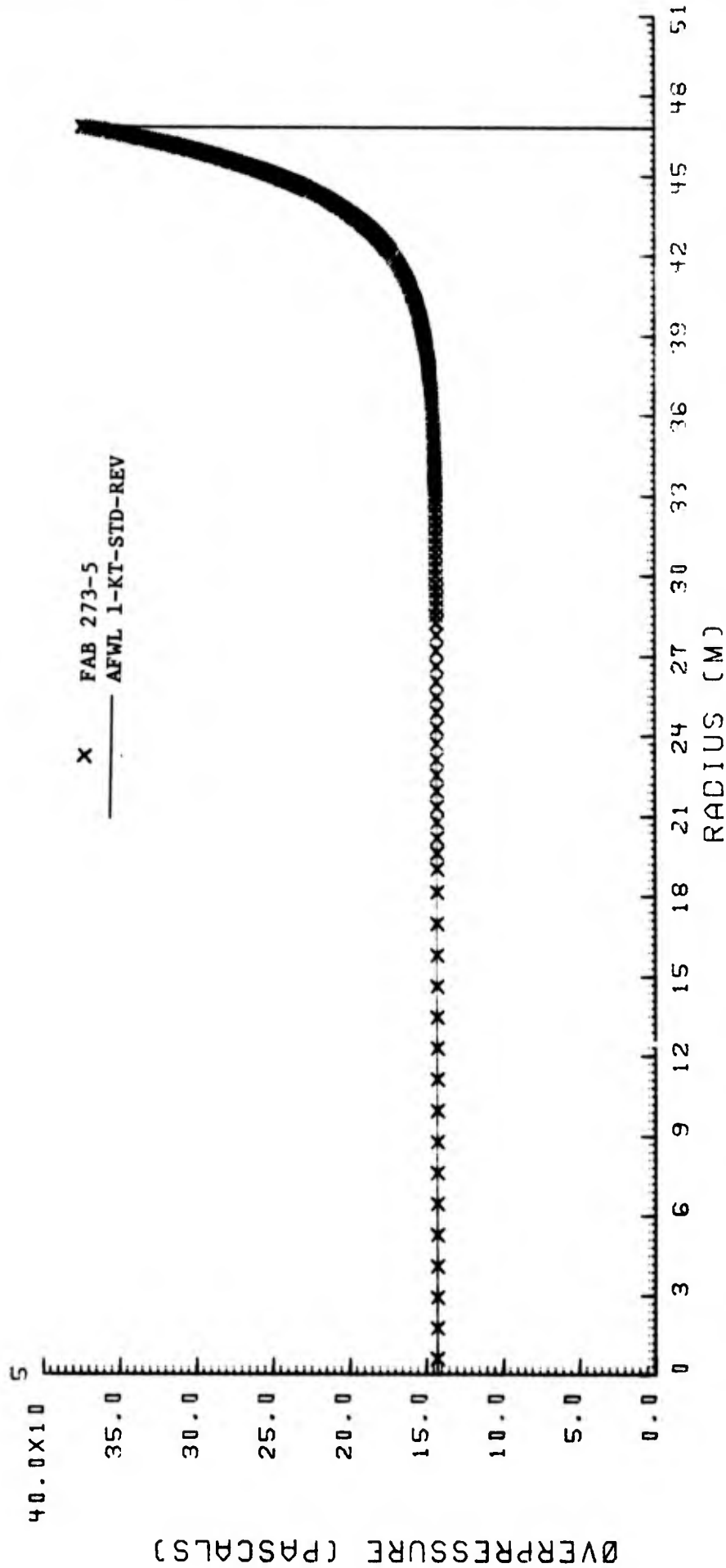


Figure 3. Comparisons of Pressure, Density and Velocity Distributions at 0.010 Seconds After Detonation.

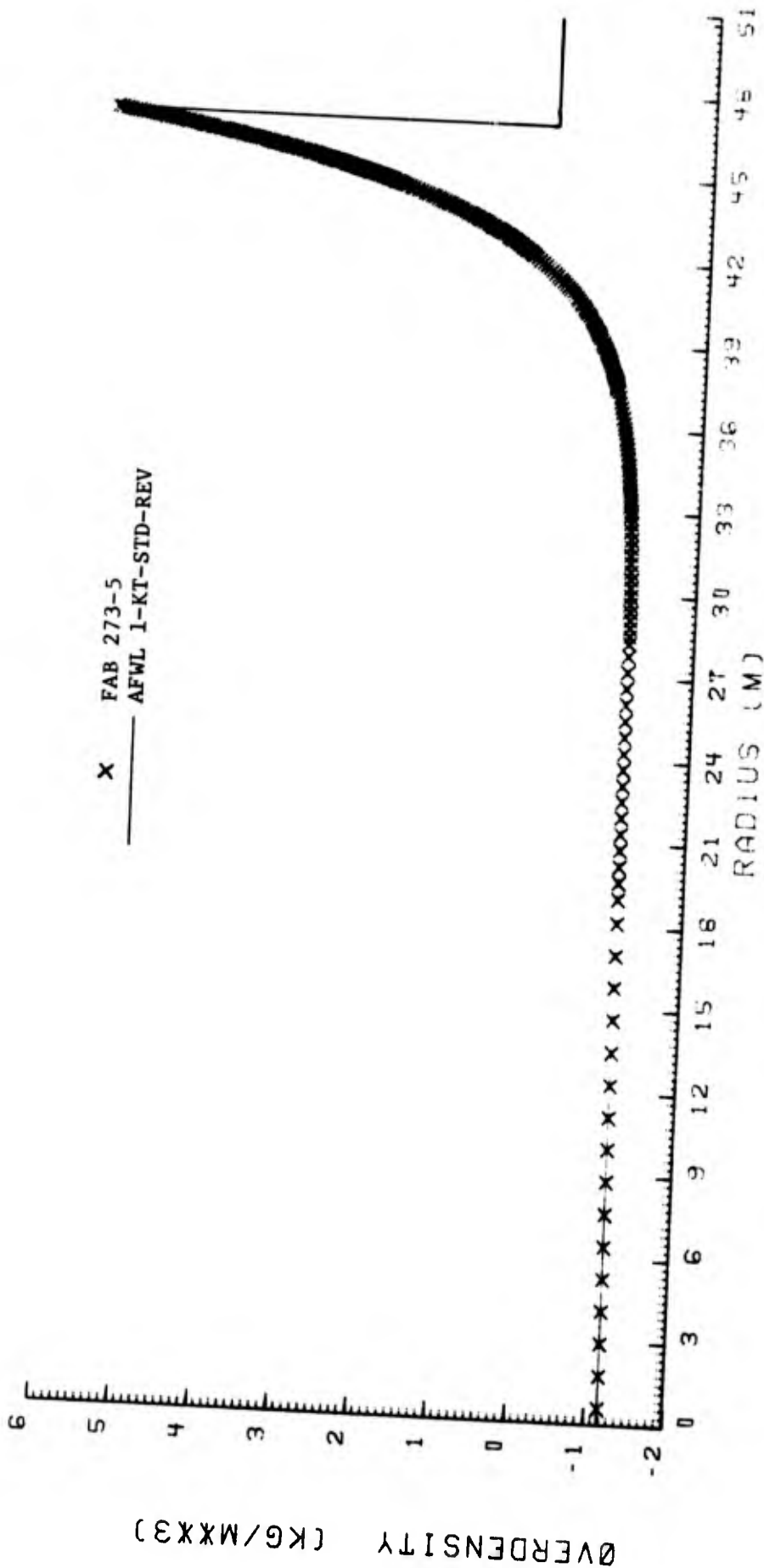


Figure 3. Continued.

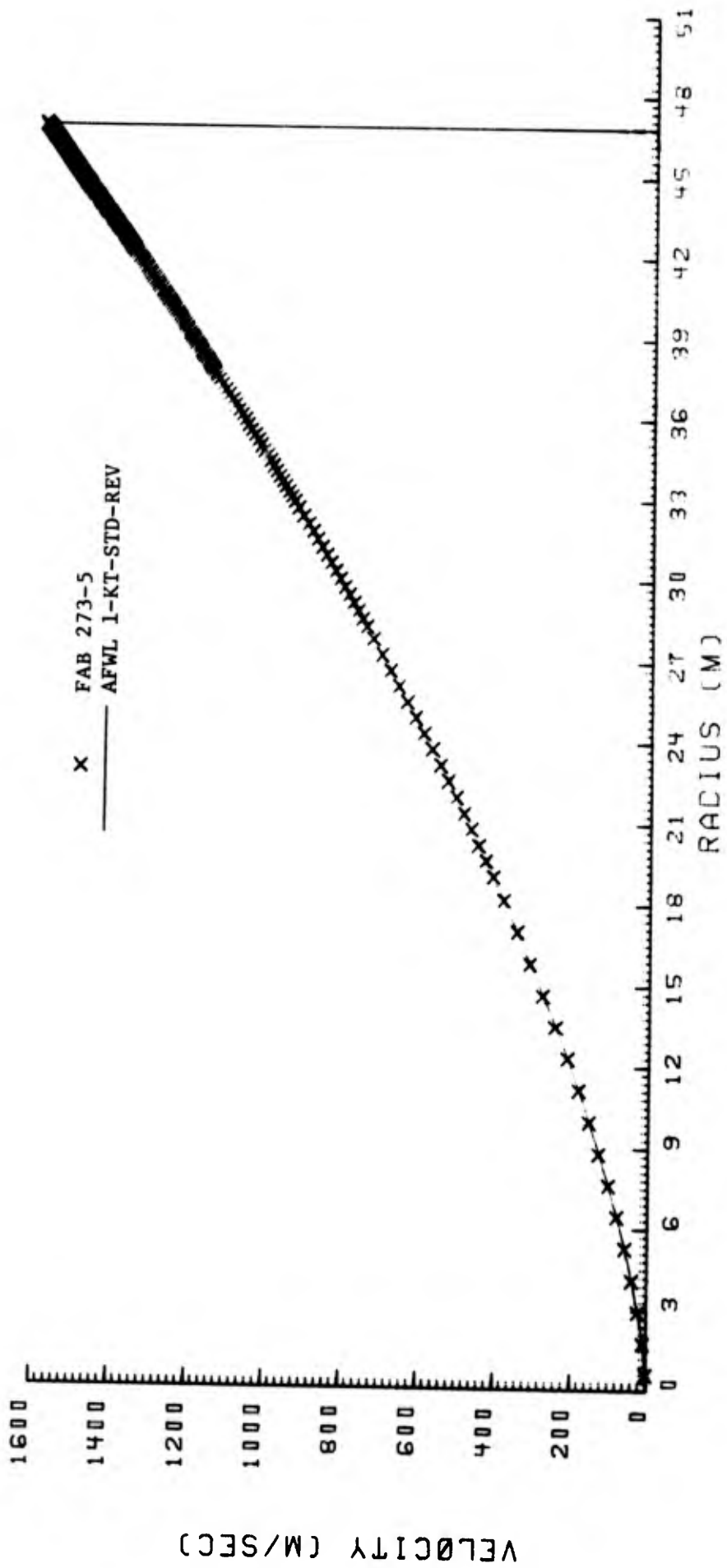


Figure 3. Concluded.

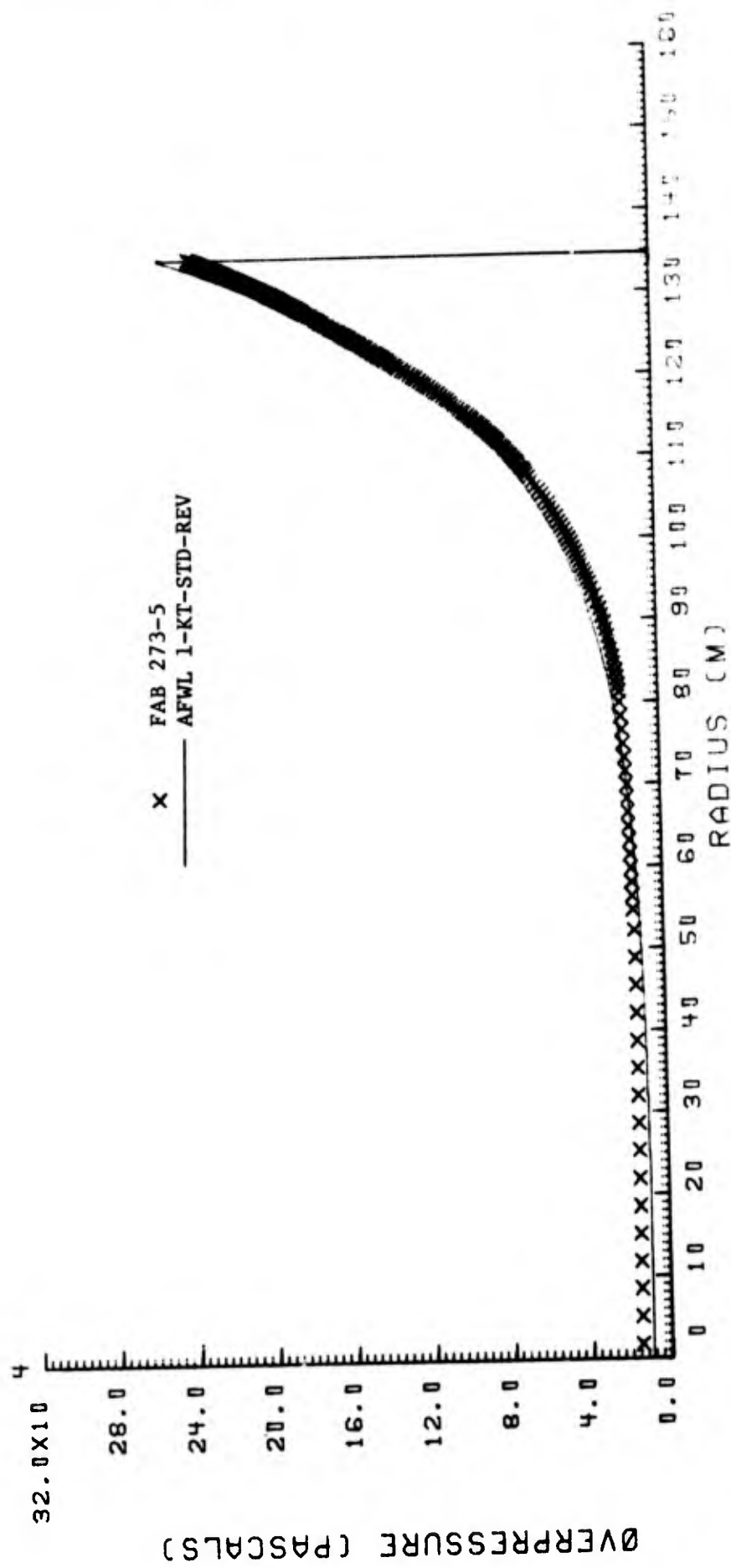


Figure 4. Comparisons of Pressure, Density and Velocity Distributions at 0.102 Seconds After Detonation.

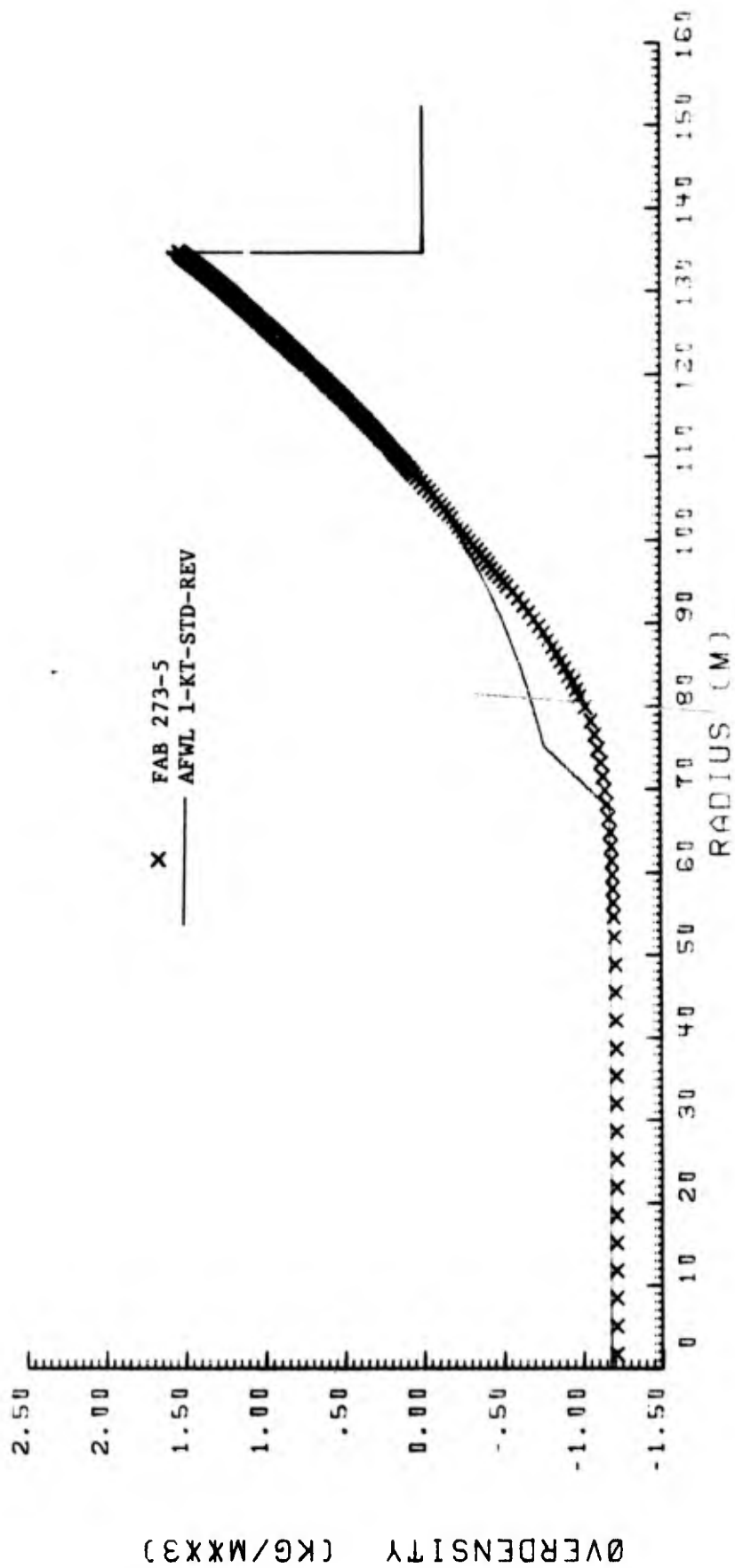


Figure 4. Continued.

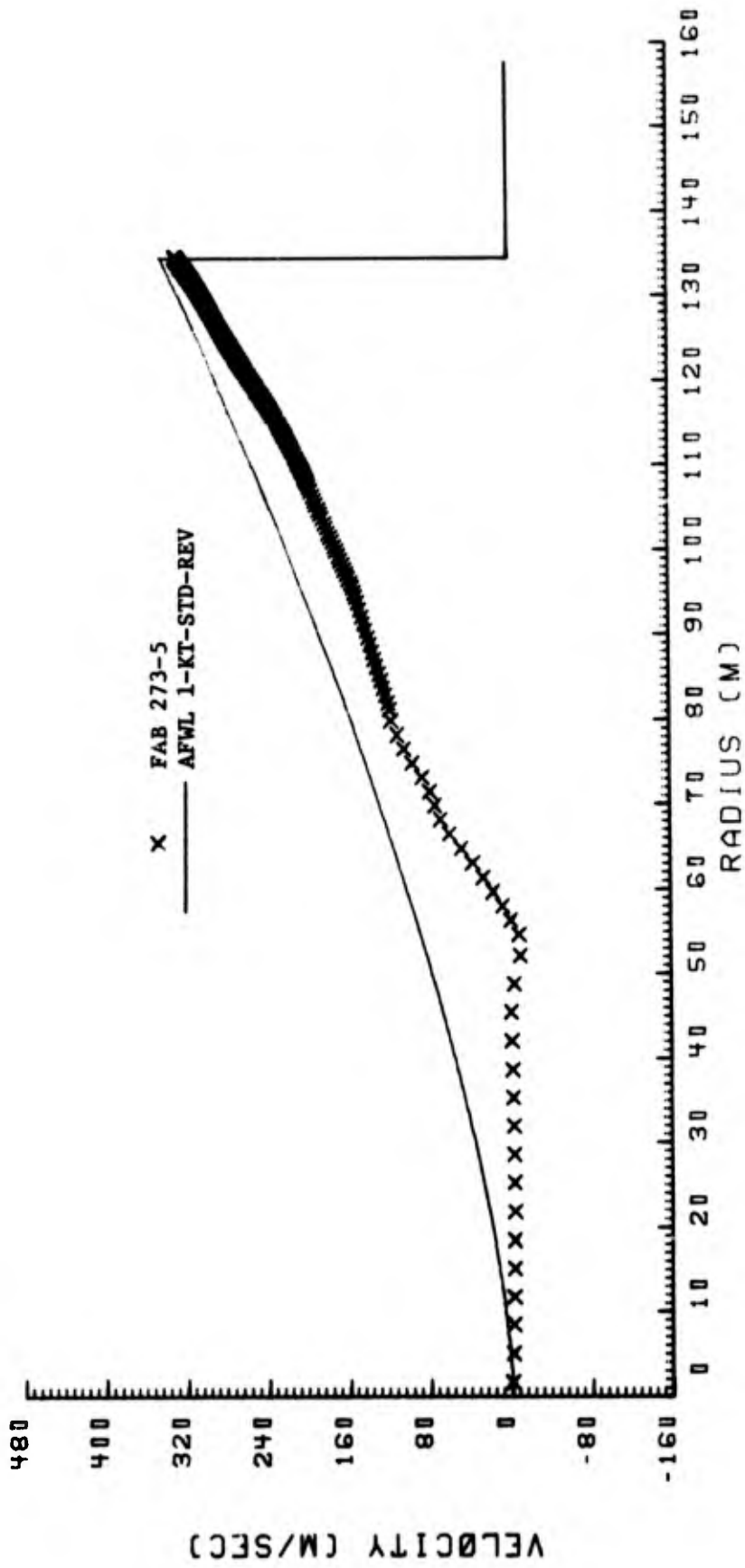


Figure 4. Concluded.

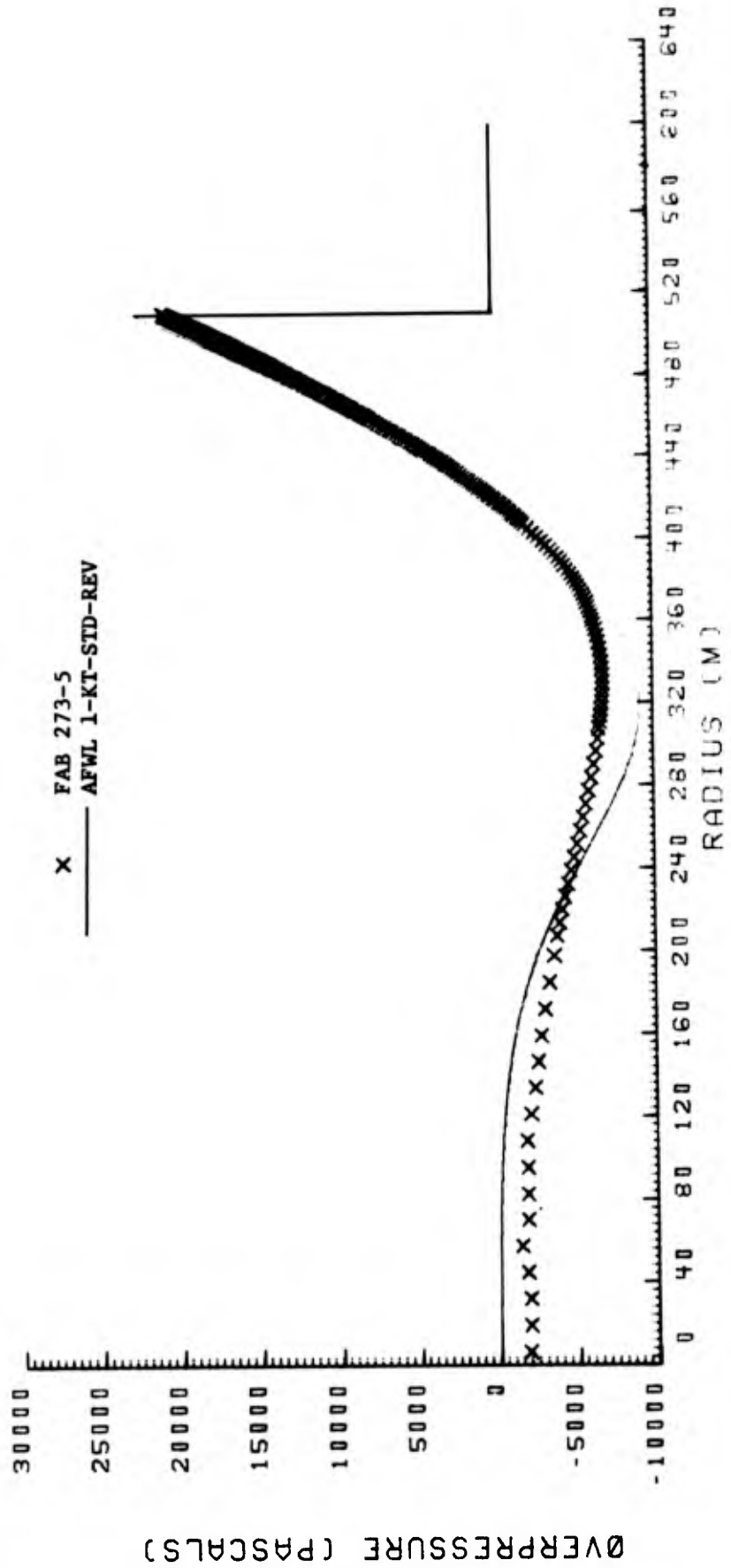


Figure 5. Comparisons of Pressure, Density and Velocity Distributions at 1.020 Seconds After Detonation.

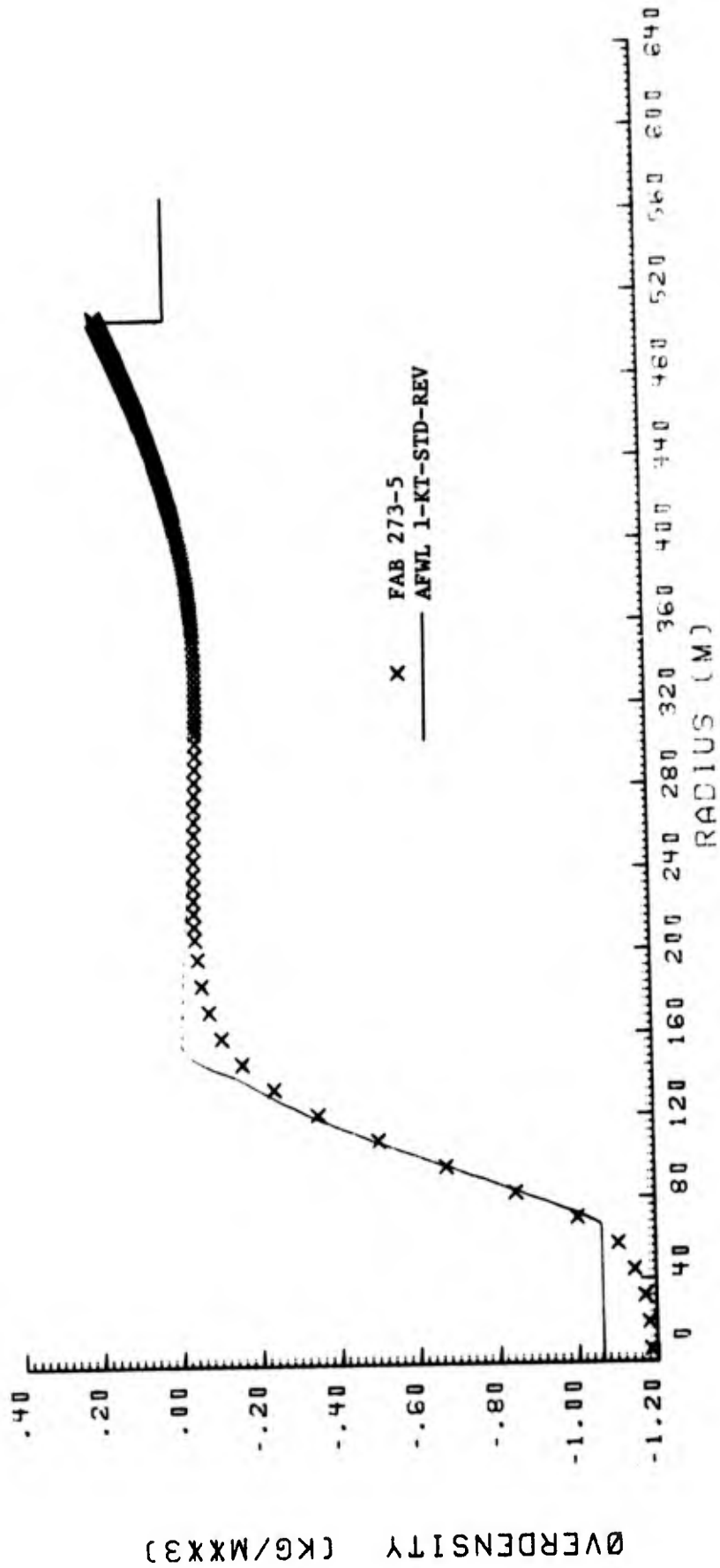


Figure 5. Continued.

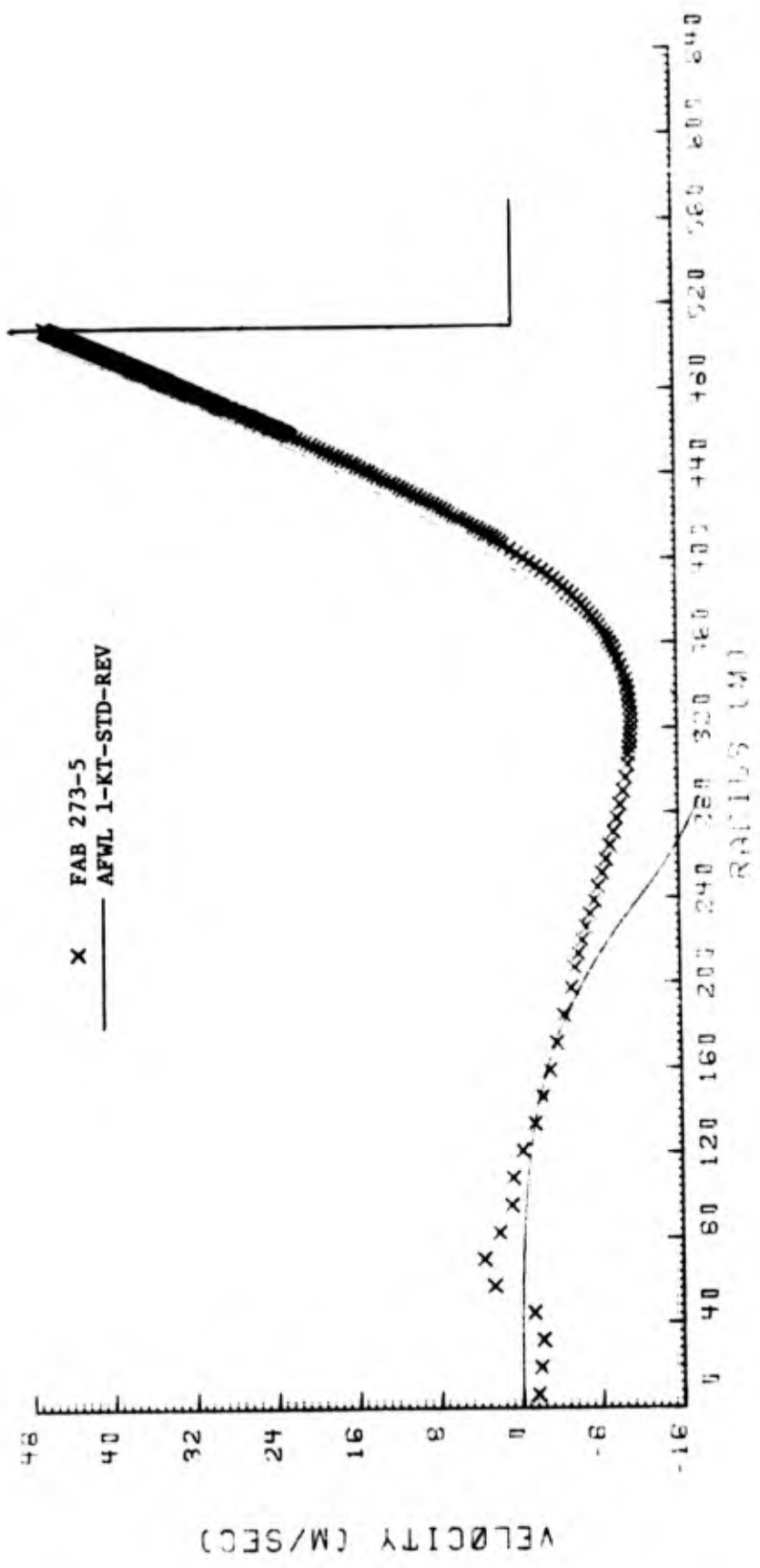


Figure 5. Concluded.

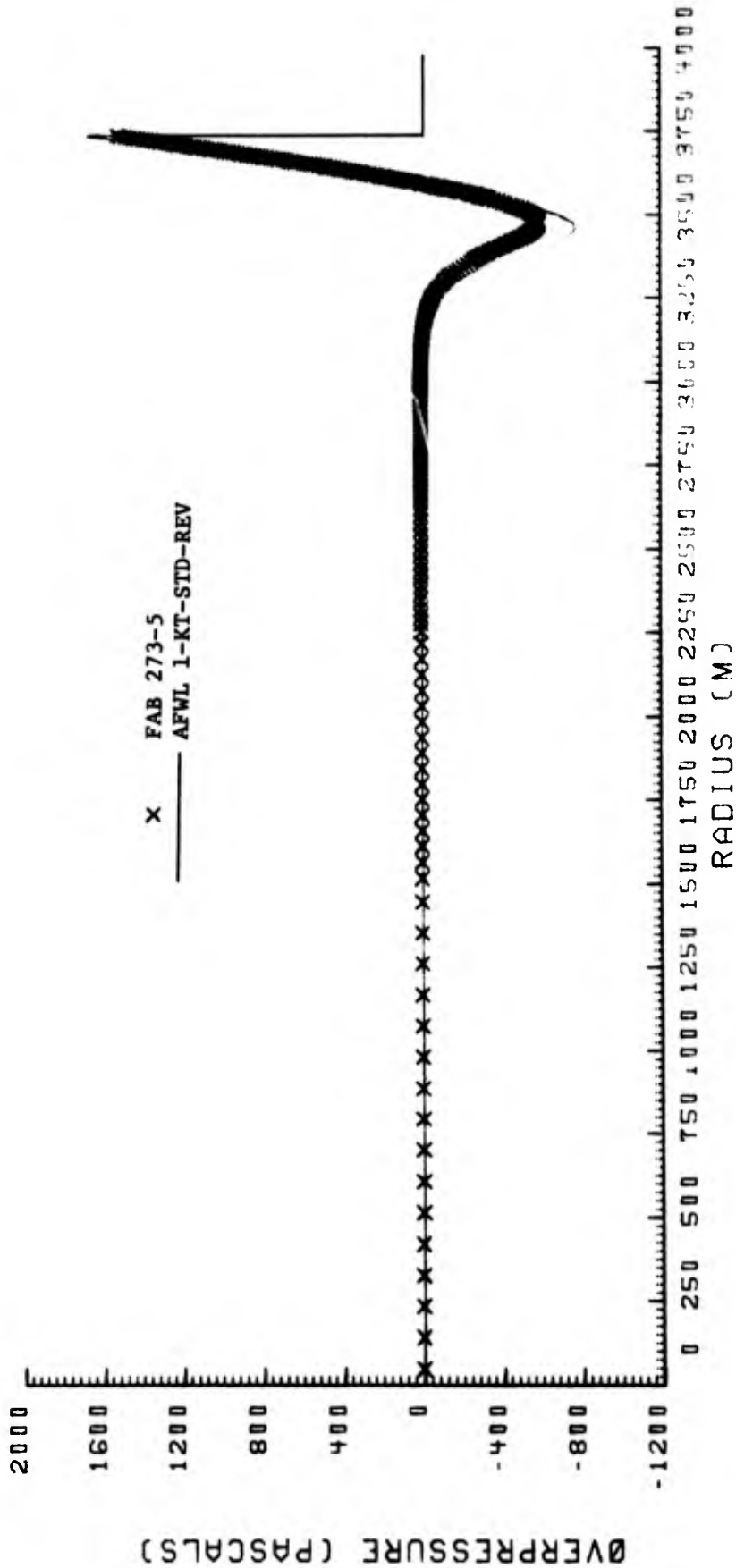


Figure 6. Comparisons of Pressure, Density and Velocity Distributions at 10.32 Seconds After Detonation.

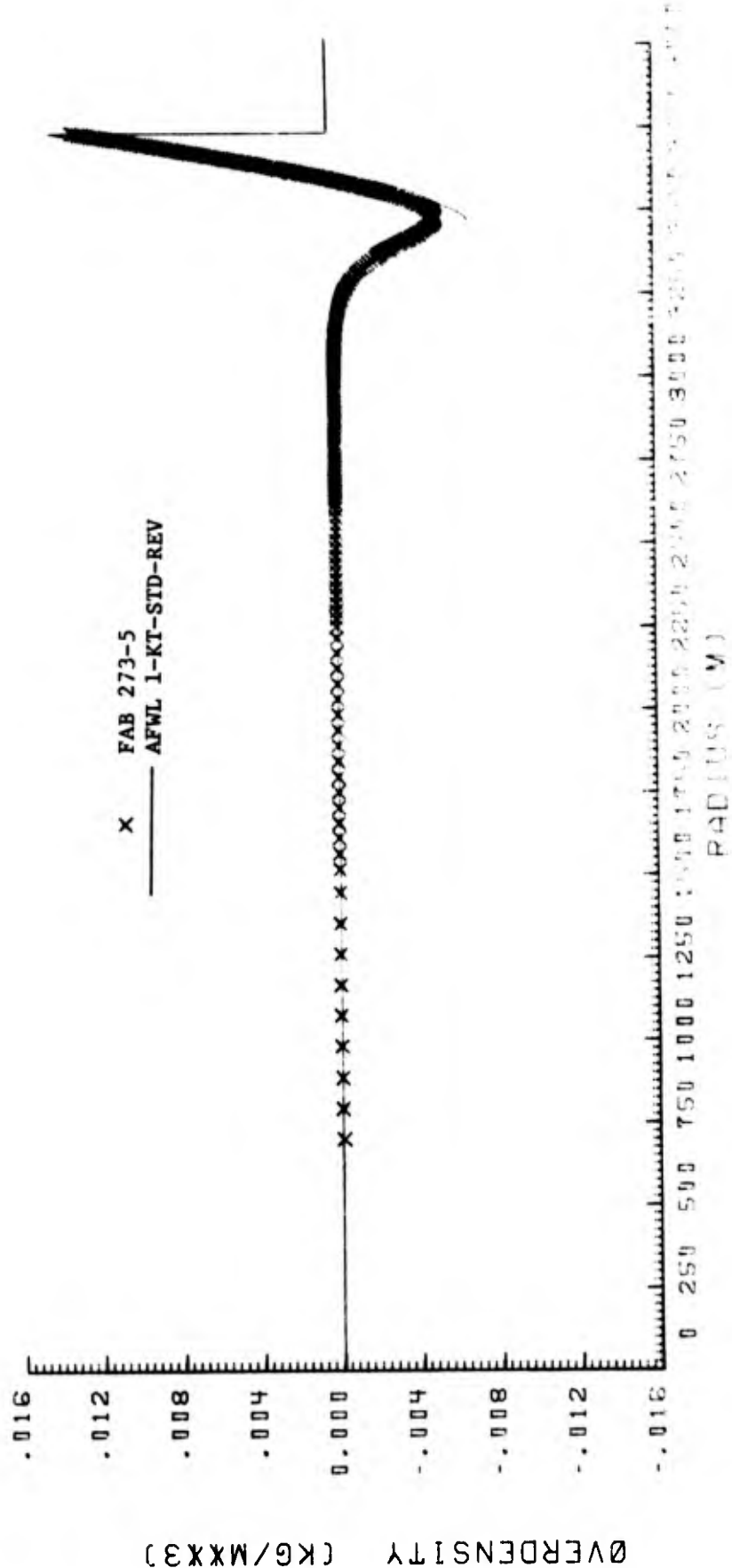


Figure 6. Continued.

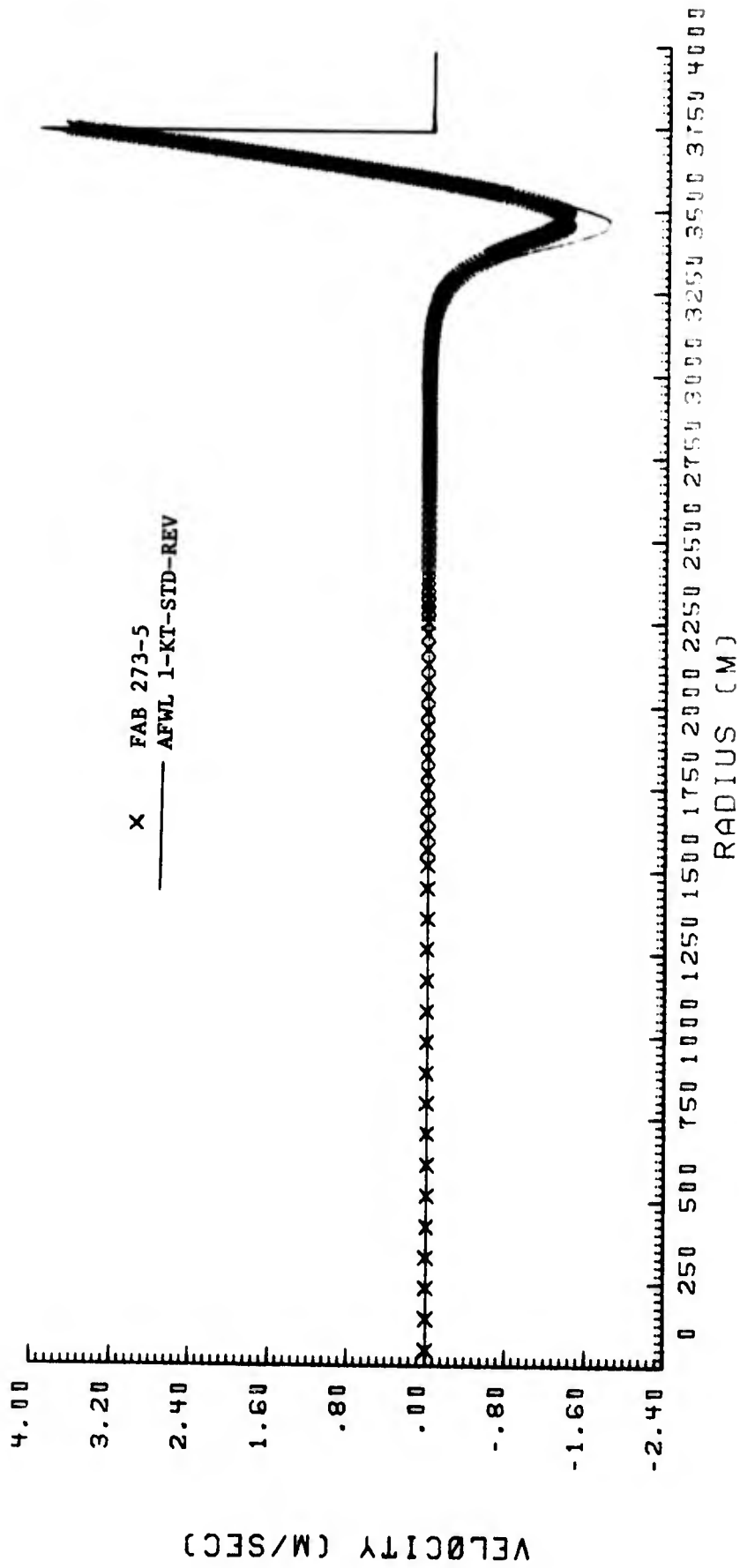


Figure 6. Concluded.

## SECTION 5

### COMPARISONS WITH OTHER PREDICTIONS AND TEST DATA

This section presents a comparison of FAB code predictions with the commonly used nuclear test data summaries, U.S.-'59-STD (Ref. 2), representing ground based measurements, and the combined Airborne-Measurement data representation given in Table 3.2-6 of Reference 2. Also compared are the predictions of the Revised AFWL 1-KT Standard (Ref. 7) and the NOL WUNDY Code (Ref. 5).

Tables 5 to 9 and Figures 2 to 6 present comparisons of the various code predictions and test data summaries for shock front radii from 175 to 50,000 feet, corresponding to overpressures from 380 to 0.04 psi.

#### 5-1 SHOCK FRONT PRESSURES.

Considering first the shock front pressures, Figure 2 and Table 5 present a comparison of shock overpressures as given by the FAB code (interpolated to the indicated radii for the table), by other prediction methods and by nuclear test data summaries.

##### 5-1.1 Equation-of-State.

Comparing the results of the FAB code results for the two different equations of state used (Brode 1965 and Doan-Nickel), it can be seen from Figure 2 or Table 5 that there is little difference in the computed overpressures using these two equations-of-state. Overpressure differences are generally below 1 percent at the highest overpressures and below about 0.02 psi at the lowest overpressures.

##### 5-1.2 Initial Conditions.

In order to determine the effect of initial blast field conditions on FAB code results, code runs were made for two different inputs (at 10 msec. after detonation), one run (134-18) with input conditions from the AFWL-1KT-STD-REV (Ref. 7) and another (134-19) with input conditions from a Sputter code run (Usertape FB21, Ref. 13).

Table 5.

## COMPARISON OF SHOCK FRONT PRESSURES

RADIUS (FT)	OVERPRESSURE (PSI)				
	U.S.-'59-STD	FAB-273-5 (BRODE EQ. STATE)	FAB-273-7 (DOAN-NICKEL EQ. STATE)	AIRBORNE MEASUREMENT POLYNOMIALS	AFWL 1-KT-STD (REV.)
175.0	360.000	371.843	371.178		379.037
200.0	246.000	257.992	256.508		263.771
225.0	186.000	186.813	186.692		192.635
250.0	144.000	141.446	141.452		146.148
275.0	107.000	110.618	110.493		114.352
300.0	88.800	88.730	88.297		91.778
325.0	73.500	72.550	71.828		75.246
350.0	62.700	60.260	59.334		62.817
375.0	54.500	50.822	49.722		53.262
400.0	46.600	43.205	42.283		45.770
450.0	36.400	32.607	31.918		34.961
500.0	29.300	25.848	25.350		27.700
550.0	24.100	21.219	20.885		22.596
600.0	20.200	17.798	17.579		18.871
650.0	17.200	15.174	15.025		16.068
700.0	14.800	13.123	13.016		13.902
750.0	12.900	11.495	11.410		12.192
800.0	11.300	10.184	10.114		10.816
850.0	9.900	9.111	9.050		9.689
900.0	8.800	8.222	8.166		8.754
950.0	7.900	7.475	7.424		7.968
1000.0	7.000	6.840	6.793	6.99	7.300
1105.0	5.630	5.772	5.739	5.95	6.183
1221.0	4.720	4.900	4.870	5.07	5.265
1350.0	3.970	4.174	4.145	4.33	4.500
1492.0	3.350	3.572	3.549	3.70	3.867
1649.0	2.830	3.067	3.048	3.18	3.335
1822.0	2.390	2.644	2.628	2.73	2.887
2014.0	2.030	2.283	2.272	2.35	2.505
2226.0	1.720	1.978	1.969	2.00	2.179
2460.0	1.470	1.718	1.712	1.75	1.901
2718.0	1.250	1.496	1.492	1.53	1.661
3004.0	1.070	1.304	1.322	1.34	1.453
3320.0	.921	1.139	1.139	1.17	1.273
3669.0	.792	.997	.998	1.03	1.117
4055.0	.682	.874	.876	0.902	.981

Table 5. Concluded.

## COMPARISON OF SHOCK FRONT PRESSURES

RADIUS (FT)	OVERPRESSURE (PSI)				
	U.S.-'59-STD	FAB-273-5 (BRODE EQ. STATE)	FAB-273-7 (DOAN-NICKEL EQ. STATE)	AIRBORNE MEASUREMENT POLYNOMIALS	AFWL 1-KT-S1D (REV.)
4482.0	.589	.767	.770	0.793	.862
4953.0	.510	.674	.678	0.698	.758
5474.0	.442	.592	.598	0.615	.667
6050.0	.385	.522	.527	0.542	.588
6686.0	.335	.460	.466	0.478	.518
7389.0	.293	.406	.412	0.422	.457
8166.0	.256	.358	.365	0.374	.403
9025.0	.225	.316	.324	0.331	.356
9974.0	.197	.282	.294	0.293	.314
11023.0	.174	.250		0.260	.278
12182.0	.154	.222		0.231	.246
13464.0	.135	.197		0.205	.218
14880.0	.121	.175		0.183	.193
16445.0	.107	.156		0.163	.171
18174.0	.096	.138		0.145	.151
20086.0	.085	.123		0.129	.134
22198.0	.076	.109		0.116	.119

Table 6.

## EFFECT OF INITIAL CONDITIONS ON SHOCK FRONT PRESSURES

RADIUS (FT)	OVERPRESSURE (PSI)	
	FAB-134-18 (1KT-STD INPUT)	FAB-134-19 (SPUTTER FB21 INPUT)
200.0	256.358	252.088
225.0	186.257	187.931
250.0	141.050	140.695
275.0	110.310	108.117
300.0	88.479	86.478
325.0	72.311	71.542
350.0	60.064	59.935
375.0	50.689	50.780
400.0	43.137	43.416
450.0	32.601	32.982
500.0	25.836	26.150
550.0	21.176	21.390
600.0	17.754	17.896
650.0	15.143	15.232
700.0	13.106	13.155
750.0	11.488	11.510
800.0	10.182	10.185
850.0	9.112	9.101
900.0	8.223	8.203
950.0	7.475	7.448
1000.0	6.839	6.808
1105.0	5.775	5.738
1221.0	4.901	4.860
1350.0	4.173	4.132
1492.0	3.570	3.530
1649.0	3.065	3.027
1822.0	2.631	2.596
2014.0	2.271	2.240
2226.0	1.966	1.938
2460.0	1.706	1.681
2718.0	1.484	1.462
3004.0	1.293	1.274
3320.0	1.129	1.112
3669.0	.987	.972
4055.0	.864	.851

Table 6. Concluded.

## EFFECT OF INITIAL CONDITIONS ON SHOCK FRONT PRESSURES

RADIUS (FT)	OVERPRESSURE (PSI)	
	FAB-134-18 (1KT-STD INPUT)	FAB-134-19 (SPUTTER FB21 INPUT)
4482.0	.757	.746
4953.0	.664	.654
5474.0	.584	.575
6050.0	.513	.506
6686.0	.452	.445
7389.0	.398	.392
8166.0	.350	.345
9025.0	.309	.304
9974.0	.276	.272
11023.0	.246	.243
12182.0	.219	.216
13464.0	.194	.191
14880.0	.172	.170
16445.0	.153	.151
18174.0	.135	.134
20086.0	.120	.119
22198.0	.107	.105
24532.0	.095	.093
27113.0	.084	.083
29964.0	.074	.074
33115.0	.066	.065
36598.0	.059	.058
40447.0	.052	.051
44701.0	.046	.046
50000.0	.040	.040

Table 7.

## EFFECT OF INITIAL CONDITIONS ON SCALED SHOCK FRONT PRESSURES

SCALED RADIUS (FT/KT <sup>1/3</sup> )	OVERPRESSURE (PSI)	
	FAB-134-18 (IKT-STD INPUT)	FAB-134-19 (SPUTTER FB21 INPUT)
200.0	249.977	253.227
225.0	181.738	188.915
250.0	137.708	141.479
275.0	107.759	108.694
300.0	86.439	86.894
325.0	70.644	71.872
350.0	58.729	60.222
375.0	49.523	51.021
400.0	42.174	43.625
450.0	31.926	33.151
500.0	25.335	26.261
550.0	20.780	21.478
600.0	17.430	17.968
650.0	14.871	15.293
700.0	12.875	13.206
750.0	11.290	11.553
800.0	10.010	10.222
850.0	8.961	9.134
900.0	8.089	8.232
950.0	7.356	7.475
1000.0	6.732	6.831
1105.0	5.687	5.757
1221.0	4.828	4.876
1350.0	4.113	4.145
1492.0	3.520	3.541
1649.0	3.023	3.036
1822.0	2.595	2.604
2014.0	2.241	2.246
2226.0	1.940	1.943
2460.0	1.684	1.686
2718.0	1.465	1.466
3004.0	1.277	1.277
3320.0	1.115	1.114
3669.0	.975	.974
4055.0	.853	.853

Table 7. Concluded.

EFFECT OF INITIAL CONDITIONS ON SCALED SHOCK FRONT PRESSURES

SCALED RADIUS (FT/KT <sup>1/3</sup> )	OVERPRESSURE (PSI)	
	FAB-134-18 (1KT-STD INPUT)	FAB-134-19 (SPUTTER FB21 INPUT)
4482.0	.748	.748
4953.0	.656	.656
5474.0	.577	.576
6050.0	.507	.507
6686.0	.446	.446
7389.0	.393	.393
8166.0	.346	.346
9025.0	.305	.305
9974.0	.273	.273
11023.0	.243	.243
12182.0	.216	.216
13464.0	.192	.192
14860.0	.170	.170
16445.0	.151	.151
18174.0	.134	.134
20086.0	.119	.119
22198.0	.105	.105
24532.0	.094	.094
27113.0	.083	.083
29964.0	.074	.074
33115.0	.065	.065
36598.0	.058	.058
40447.0	.051	.051
44701.0	.046	.046
50000.0	.040	.040

Table 8.

## EFFECTS OF THERMAL RADIATION ON SHOCK FRONT PRESSURES

RADIUS (FT)	OVERPRESSURE (PSI)			
	RADIATION	NO RADIATION		AFWL 1-KT-STD-REV
	FAB-134-18	FAB-134-21	NOL	
175.0	370.997	370.998	386.624	379.037
200.0	256.358	256.358	268.015	263.771
225.0	186.257	186.258	202.266	192.635
250.0	141.050	141.069	151.850	146.148
275.0	110.310	110.431	118.717	114.352
300.0	88.479	88.771	93.316	91.778
325.0	72.311	72.712	76.126	75.246
350.0	60.064	60.502	63.105	62.817
375.0	50.689	51.164	53.960	53.262
400.0	43.137	43.649	46.747	45.770
450.0	32.601	33.287	36.029	34.961
500.0	25.836	26.703	28.757	27.700
550.0	21.176	22.025	23.431	22.596
600.0	17.754	18.485	19.616	18.871
650.0	15.143	15.780	16.602	16.068
700.0	13.106	13.677	14.458	13.902
750.0	11.488	12.012	12.730	12.192
800.0	10.182	10.657	11.309	10.816
850.0	9.112	9.562	10.141	9.689
900.0	8.223	8.642	9.056	8.754
950.0	7.475	7.865	8.208	7.968
1000.0	6.839	7.202	7.554	7.300
1105.0	5.775	6.090	6.386	6.183
1221.0	4.901	5.173	5.375	5.265
1350.0	4.173	4.408	4.576	4.500
1492.0	3.570	3.773	3.912	3.867
1649.0	3.065	3.240	3.336	3.335
1822.0	2.631	2.785	2.818	2.887
2014.0	2.271	2.402	2.432	2.505
2226.0	1.966	2.079	2.131	2.179
2460.0	1.706	1.804	1.835	1.901
2718.0	1.484	1.570	1.605	1.661
3004.0	1.293	1.368	1.403	1.453
3320.0	1.129	1.194	1.232	1.273
3669.0	.987	1.043	1.075	1.117
4055.0	.864	.913	0.948	.981

Table 8. Concluded.

## EFFECTS OF THERMAL RADIATION ON SHOCK FRONT PRESSURES

RADIUS (FT)	OVERPRESSURE (PSI)			
	RADIATION	NO RADIATION		AFWL 1-KT-STD-REV
	FAB-134-18	FAB-134-21	NOL	
4482.0	.757	.801	.834	.862
4953.0	.664	.703	.735	.758
5474.0	.584	.617	.644	.667
6050.0	.513	.543	.568	.588
6686.0	.452	.478	.501	.518
7389.0	.398	.421	.443	.457
8166.0	.350	.371	.391	.403
9025.0	.309	.327	.346	.356
9974.0	.276	.290	.307	.314
11023.0	.246	.259	.272	.278
12182.0	.219	.231	.241	.246
13464.0	.194	.205	.213	.218
14880.0	.172	.182	.189	.193
16445.0	.153	.161	.167	.171
18174.0	.135	.143	.148	.151
20086.0	.120	.127	.132	.134
22198.0	.107	.113	.117	.119
24532.0	.095	.100	.104	.106
27113.0	.084	.089	.092	.094
29964.0	.074	.079	.081	.084
33115.0	.066	.070	.072	.074
36598.0	.059	.062	.064	.066
40447.0	.052	.055	.058	.059
44701.0	.046	.049	.051	.052
50000.0	.040	.043	.045	.046

Table 9.

## COMPARISON OF SHOCK ARRIVAL TIMES

RADIUS (FT)	SHOCK ARRIVAL TIME (SECONDS)				
	U.S.-'59-STD	FAB-273-5 (BRODE EQ. STATE)	FAB-273-7 (DOAN-NICKEL EQ. STATE)	AIRBORNE MEASUREMENT POLYNOMIALS	AFWL 1-KT-STD (REV.)
175.0	.01432	.01378	.01379		.01370
200.0	.01954	.01894	.01895		.01883
225.0	.02555	.02509	.02510		.02482
250.0	.03235	.03206	.03207		.03168
275.0	.04032	.03985	.03987		.03941
300.0	.04903	.04847	.04851		.04799
325.0	.05844	.05793	.05801		.05741
350.0	.06853	.06813	.06828		.06762
375.0	.07924	.07905	.07930		.07857
400.0	.09055	.09064	.09103		.09021
450.0	.11481	.11576	.11640		.11441
500.0	.14105	.14306	.14396		.14110
550.0	.16905	.17216	.17329		.16957
600.0	.19860	.20284	.20418		.19925
650.0	.22955	.23487	.23638		.23013
700.0	.26173	.26801	.26967		.26240
750.0	.29501	.30222	.30403		.29623
800.0	.32929	.33727	.33922		.33111
850.0	.36445	.37313	.37521		.36686
900.0	.40041	.40961	.41183		.40339
950.0	.43710	.44673	.44908		.44059
1000.0	.47444	.48437	.48684	.474	.47838
1105.0	.55500	.56479	.56755	.554	.55935
1221.0	.64600	.65560	.65865	.645	.65102
1350.0	.74900	.75837	.76174	.747	.75484
1492.0	.86400	.87326	.87698	.861	.87095
1649.0	.99400	1.00201	1.00611	.990	1.00104
1822.0	1.14000	1.14550	1.15000	1.13	1.14599
2014.0	1.30000	1.30632	1.31125	1.29	1.30836
2226.0	1.48000	1.48541	1.49081	1.48	1.48908
2460.0	1.68000	1.68457	1.69047	1.68	1.68990
2718.0	1.90000	1.90555	1.91199	1.90	1.91244
3004.0	2.15000	2.15187	2.15891	2.14	2.16065
3320.0	2.43000	2.42533	2.43299	2.42	2.43603
3669.0	2.73000	2.72862	2.73695	2.72	2.74128
4055.0	3.07000	3.06528	3.07436	3.06	3.07993

Table 9. Concluded.

## COMPARISON OF SHOCK ARRIVAL TIMES

RADIUS (FT)	SHOCK ARRIVAL TIME (SECONDS)				
	U.S.-'59-STD	FAB-273-5 (BRODE EQ. STATE)	FAB-273-7 (DOAN-NICKEL EQ. STATE)	AIRBORNE MEASUREMENT POLYNOMIALS	AFWL 1-KT-STD (REV.)
4482.0	3.45000	3.43890	3.44877	3.43	3.45555
4953.0	3.86000	3.85216	3.86290	3.84	3.87086
5474.0	4.32000	4.31041	4.32208	4.30	4.33120
6050.0	4.83000	4.81812	4.83080	4.81	4.84105
6686.0	5.40000	5.37976	5.39354	5.37	5.40490
7389.0	6.02000	6.00160	6.01655	5.99	6.02902
8166.0	6.71000	6.68988	6.70609	6.68	6.72050
9025.0	7.47000	7.45178	7.46934	7.44	7.48532
9974.0	8.32000	8.29447	8.31355	8.28	8.33114
11023.0	9.25000	9.22688		9.22	9.26694
12182.0	10.29000	10.25795		10.25	10.30171
13464.0	11.43000	11.39932		11.39	11.44714
14880.0	12.69000	12.66085		12.65	12.71311
16445.0	14.09000	14.05597		14.04	14.11310
18174.0	15.64000	15.59811		15.59	15.66061
20086.0	17.34000	17.30429		17.29	17.37270
22198.0	19.23000	19.18973		19.18	19.26467

The initial pressure distribution and total energy for these two input conditions were about the same, but the absolute densities and temperatures were considerably different in some regions of the blast field, by about a factor of two near the center of the blast field. Overpressures obtained from these two FAB runs, interpolated to the same radii conditions, are compared in Table 6.

The overpressures for the two input calculations in Table 6 are seen to differ slightly, with differences generally being less than 2 percent. For low overpressures below about 3 psi the difference can be attributed to the about 3 percent yield differences for the two runs (see Table 1). If the code results for these two runs are reduced by standard cube root scaling to a 1-KT basis, as presented in Table 7, the code results for the two different inputs are seen to be essentially identical for overpressures below about 4 psi.

#### 5-1.3 Comparisons with Nuclear Test Data Summaries.

The FAB shock overpressure results are compared in Figure 2 and Table 5 with the nuclear test data summaries presented in Reference 2, the U.S.-'59-STD and an Airborne-Measurement Summary (Tables 3.2-7 and 3.2-6, respectively, of Ref. 2). Also shown for comparison are the AFWL revised 1-KT-STD values. The columns in Table 5 are arranged from left to right in order of ascending shock overpressure at the 1 psi level.

The FAB initial conditions, as mentioned, were generally taken from the AFWL 1-KT-STD-REV values at 0.010 seconds, when the blast radius is 153.6 ft.

At a shock radius of 175 ft (360 psi), the shock overpressure for the FAB results with the Brode equation of state is 3 percent higher than the U.S.-'59-STD value. The 1-KT-STD-REV value is 5 percent above the U.S.-'59-STD value. At a 600 ft blast radius (about 20 psi) the 1-KT-STD-REV and FAB (Brode eq. state) values are respectively 7 and 13 percent below the U.S.-'59-STD values. Below about 20 psi shock overpressure the FAB (Brode eq. state) and 1-KT-STD-REV values increase relative to the U.S.-'59-STD values, being in good agreement at 1000 ft (7 psi) where they are respectively 2 percent below and 4 percent above.

The Airborne Measurement shock overpressure value from Reference 2 is in agreement with the U.S.-'59-STD value at 1000 ft (7 psi). In the overpressure range below 7 psi the U.S.-'59-STD values decrease markedly relative to the Airborne Measurement values. At 2226, 3669 and 14,880 ft where the airborne data are respectively 2.00, 1.03 and 0.183 psi, the U.S.-'59-STD values are respectively 14, 23 and 34 percent less. In this low shock overpressure range from 2 to 0.18 psi the FAB results are only 1 to 4 percent below the airborne data and the 1-KT-STD values are 5 to 9 percent higher than the airborne data.

Predictions of the NOL WUNDY code, shown in Figure 2 (see also Table 8), like those for the AFWL 1-KT-STD-REV, exceed the nuclear test data summaries for overpressures below about 7 psi, due in part to neglect of thermal radiation in the WUNDY code, as is discussed below.

#### 5-1.4 Thermal Radiation.

Since some free-air burst codes such as the NOL WUNDY code do not take into account thermal radiation, it appeared useful to make FAB code runs with and without consideration of thermal radiation to evaluate the importance of this radiation effect. Results of these runs are presented in Table 8 together with predictions of the NOL WUNDY code and the AFWL 1-KT-STD-REV. It is evident by comparison of the FAB results in this table that if thermal radiation is neglected the predicted overpressures are generally about 5 percent too high in the below 10 psi overpressure range. With regard to the NOL WUNDY predictions, which neglect thermal radiation, this observation suggests that the NOL predictions can be expected to be about 5 percent too high in the below 10 psi overpressure range. This suggestion is also supported by the fact that the no-radiation FAB results in Table 9 (for Run 134-21) are in much better agreement with the NOL predictions than are the FAB results with radiation taken into account.

#### 5-1.5 Shock Arrival Time.

Shock arrival time according to the various predictions and test data are compared in Table 9 for ranges from 175 to 22,198 feet. Generally all predicted arrival times are seen to be in reasonable agreement with each other and with the test data summaries.

Overpressure, overdensity and material velocity distributions from the FAB code (Run 573-5) are compared with the corresponding distributions of the AFWL Revised 1-KT Standard in Figures 4 to 6 for times of shock arrival of about 0.1, 1 and 10 seconds after detonation. (The initial conditions for this FAB run were taken from the 1-KT-STD-REV distributions presented in Figure 3 for 0.01 second after detonation.) These distributions correspond to shock front overpressure levels of 34, 3.0 and 0.22 psi (or 235, 21 and 1.5 kilopascals), respectively, at shock radii of 441, 1671 and 12,252 ft (or 135, 509 and 3734 meters).

The two sets of distributions shown in Figures 4 to 6 are seen to be in reasonably good agreement with each other in most respects. Some noticeable differences are seen particularly in the overpressure and velocity distributions at 0.1 and 1 second after detonation (34 and 3 psi shock front overpressure levels) but in the absence of an absolute test data standard, no conclusion can be drawn from this comparison as to which set of distributions is more realistic.

## SECTION 6

### CONCLUSIONS

The FAB hydrodynamic computer code has been developed to compute the blast flow characteristics of a nuclear free-air burst. Runs made with this code for a 1-KT burst at sea level and comparisons of code results with other predictions and nuclear test data summaries indicate the following conclusions.

1. The shock front overpressures predicted by the FAB code are generally close to or between the overpressures for the two groups of nuclear test data summaries as represented by the U.S.-'59-STD and the combined airborne measurement polynomials in DASA 1200.
2. The shock overpressure at a range of 1000 feet is essentially 7.00 psi according to both the U.S.-'59 empirical curve and the airborne measurement polynomials of DASA 1200. The FAB results, using the Brode (1965) equation-of-state, and the AFWL 1-KT-Standard (Revised) function essentially agree with these data, being respectively only 2 percent lower and 4 percent higher. At ranges from 2,226 to 14,880 feet, where the shock overpressure is 2.00 to 0.183 psi according to the airborne measurement data, the U.S.-'59 standard is 14 to 34 percent below the corresponding airborne value. The FAB results in this range are 1 to 4 percent lower than the airborne measurement values and the AFWL 1-KT-Standard (Rev.) values are 5 to 9 percent higher.
3. FAB shock front overpressure calculations using two different air equations-of-state (Brode 1965 and Doan-Nickel) give essentially the same results.

4. FAB shock front overpressures computed from different initial conditions (using inputs from AFWL 1-KT-STD-REV and Sputter FB21, for 0.010 seconds after detonation) give somewhat different results for early times, differences generally below 2 percent, but are in excellent agreement for overpressures below about 4 psi.
5. Comparison of FAB results with NOL WUNDY results indicates that the major differences may be attributed to the neglect of thermal radiation in the WUNDY code. It is shown that WUNDY predictions of shock front overpressures are probably about 5 percent too high at overpressures below 10 psi due to the omission of thermal radiation.

## SECTION 7

### REFERENCES

1. Brode, H.L., Point Source Explosion in Air, RAND Corp. RM-1824-AEC, December 1956. (See also: Brode, H.L., Space Plots of Pressure, Density and Particle Velocity for the Blast Wave from a Point Source in Air, RM-1824-AEC, June 1975.)
2. Ellis, P.A., et al, Nuclear Weapons Blast Phenomena, Volume 1 - Source and Development of Blast Waves in Air (U), General Electric - TEMPO, Unpublished.
3. Fry, M.A., et al., The HULL Hydrodynamics Computer Code, AFWL-TR-76-183, September 1976.
4. Lehto, D., and Lutzky, M., One-Dimensional Hydrodynamic Code for Nuclear-Explosion Calculations, NOLTR 62-168, DASA-1518, March 1965.
5. Lehto, D.L., and Larson, R.A., Long Range Propagation of Spherical Shockwaves from Explosions in Air, NOLTR 69-88, July 1969.
6. McNamara, W., Jordano, R.J., and Lewis, P.S., Air Blast from a 1 KT Nuclear Burst at 60 Metres over an Ideal Surface, General Electric-TEMPO, BRL Contract Report 353, November 1977.
7. Needham, C.E., Havens, M.L., and Knauth, C.S., Nuclear Blast Standard (1KT), AFWL-TR-73-55 (REV), April 1975.
8. Thompson, J.H., REFLECT Computer Code for Ground-Reflected Blast Waves, Kaman Avidyne Report TR-96, Defense Nuclear Agency Report No. 3470F-2, Vol. II, Computer Program Description, 21 April 1975.
9. Godunov, S.K., A Difference Method for Numerical Calculation of Discontinuous Solution of the Equations of Hydrodynamics, Mat. Sb. 47, p. 271-306, 1959.
10. Holt, M., Numerical Methods in Fluid Dynamics, Springer-Verlag, New York, 1977.
11. Brode, H.L., Theoretical Description of the Fireball, Blast and Thermal Radiation from a Nuclear Explosion at 60,000 Ft., RAND Corporation, Unpublished.
12. Sharp, A.L., A Thermal Source Model from SPUTTER Calculations, AFWL-TR-72-49, March 1973.
13. McNamara, W., Smoothed output from SPUTTER Usertape FB21 at 0.01 sec. after burst, Letter and data sent to J.R. Ruetenik, Kaman Avidyne, on 17 July 1978.

## DISTRIBUTION LIST

### DEPARTMENT OF DEFENSE

Assistant to the Secretary of Defense  
Atomic Energy  
ATTN: Executive Assistant

Defense Intelligence Agency  
ATTN: DB-4C, V. Fratzke

Defense Nuclear Agency  
ATTN: SPAS  
ATTN: STSP  
4 cy ATTN: TITL

Defense Technical Information Center  
12 cy ATTN: DD

Field Command  
Defense Nuclear Agency  
ATTN: FCT, W. Tyler  
ATTN: FCPR

Field Command  
Defense Nuclear Agency  
ATTN: FCPRL

NATO School, SHAPE  
ATTN: U.S. Documents Officer

Undersecretary of Def for Rsch & Engrg  
Department of Defense  
ATTN: Strategic & Space Systems (OS)

### DEPARTMENT OF THE ARMY

Harry Diamond Laboratories  
Department of the Army  
ATTN: DELHD-N-P, J. Gwaltney

U.S. Army Ballistic Research Labs  
ATTN: DRDAR-BLT, W. Taylor  
ATTN: DRDAR-BLT, J. Keefer

U.S. Army Materiel Dev & Readiness Cmd  
ATTN: DRCDE-D, L. Flynn

U.S. Army Nuclear & Chemical Agency  
ATTN: Library

### DEPARTMENT OF THE NAVY

Headquarters  
Naval Material Command  
ATTN: MAT OBT-22

Naval Research Laboratory  
ATTN: Code 2627

Naval Surface Weapons Center  
ATTN: Code F31, K. Caudle

Naval Weapons Evaluation Facility  
ATTN: L. Oliver

Office of Naval Research  
ATTN: Code 465

### DEPARTMENT OF THE NAVY (Continued)

Strategic Systems Project Office  
Department of the Navy  
ATTN: NSP-272

### DEPARTMENT OF THE AIR FORCE

Aeronautical Systems Division  
Air Force Systems Command  
ATTN: ASD/ENFT, R. Bachman  
4 cy ATTN: ASD/ENFTV, D. Ward

Air Force Aero-Propulsion Laboratory  
ATTN: TBC, M. Stibich

Air Force Materials Laboratory  
ATTN: MBE, G. Schmitt

Air Force Weapons Laboratory  
Air Force Systems Command  
ATTN: NTV, A. Sharp  
ATTN: SUL  
ATTN: NTV, G. Campbell

Assistant Chief of Staff  
Studies & Analyses  
Department of the Air Force  
ATTN: AF/SASB, R. Mathis

Deputy Chief of Staff  
Research, Development, & Acq  
Department of the Air Force  
ATTN: AFRD-P, N. Alexandrow

Foreign Technology Division  
Air Force Systems Command  
ATTN: SDBF, S. Spring

Strategic Air Command  
Department of the Air Force  
ATTN: XPFS, B. Stephan  
ATTN: XPFS, F. Tedesco

### DEPARTMENT OF ENERGY CONTRACTORS

Los Alamos National Scientific Laboratory  
ATTN: MS 670, J. Hopkins

Sandia National Laboratories  
ATTN: A. Lieber

### OTHER GOVERNMENT

Central Intelligence Agency  
ATTN: OSWR/NED

### DEPARTMENT OF DEFENSE CONTRACTORS

Aptek  
ATTN: T. Meagher

AVCO Research & Systems Group  
ATTN: J. Patrick  
ATTN: P. Grady

**PRECEDING PAGE BLANK-NOT FILMED**

DEPARTMENT OF DEFENSE CONTRACTORS (Continued)

BDM Corp  
ATTN: C. Somers

Boeing Co  
ATTN: M/S 35/20, E. York

Boeing Wichita Co  
ATTN: R. Syring

Calspan Corp  
ATTN: M. Dunn

University of Dayton  
Industrial Security Super KL-505  
ATTN: B. Wilt

Effects Technology, Inc  
ATTN: E. Bick  
ATTN: R. Wengler  
ATTN: R. Globus

General Electric Company—TEMPO  
ATTN: J. Moulton  
ATTN: DASIAC

General Electric Company—TEMPO  
ATTN: J. Moulton

General Research Corp  
ATTN: T. Stathacopoulos  
ATTN: J. Cunningham

Kaman Sciences Corp  
ATTN: D. Sachs

DEPARTMENT OF DEFENSE CONTRACTORS (Continued)

Kaman Avidyne  
ATTN: R. Ruetenik  
ATTN: E. Criscione  
ATTN: N. Hobbs  
ATTN: B. Lee

Los Alamos Technical Associates, Inc  
ATTN: C. Sparling  
ATTN: P. Hughes

McDonnell Douglas Corp  
ATTN: J. McGrew

Prototype Development Associates, Inc  
ATTN: J. McDonald  
ATTN: C. Thacker  
ATTN: H. Moody

R & D Associates  
ATTN: F. Field  
ATTN: J. Carpenter  
ATTN: C. MacDonald  
ATTN: A. Kuhl  
ATTN: P. Haas

Rockwell International Corp  
ATTN: R. Moonan

Science Applications, Inc  
ATTN: W. Layson